

## Reviewed Preprint

v1 • June 12, 2026

Not revised

## ✉ For correspondence:

[yingcai@zju.edu.cn](mailto:yingcai@zju.edu.cn)

\* These authors contribute equally

**Competing interests:** No competing interests declared**Funding:** See [page 25](#)**Reviewing editor:** Anna C Schapiro, University of Pennsylvania, United States

© 2026, Liu et al. This article is distributed under the terms of the [Creative Commons Attribution License](#), which permits unrestricted use and redistribution provided that the original author and source are credited.

# Ramping-up hippocampal ripples and their neocortical coupling support human visual short-term memory

Jing Liu<sup>1,2,\*</sup>, Xianhui He<sup>3,4,\*</sup>, Can Yang<sup>3</sup>, Nikolai Axmacher<sup>5</sup>, Gui Xue<sup>6,7</sup>, Shaoming Zhang<sup>8,9</sup>, Ying Cai<sup>3,10</sup> ✉

<sup>1</sup>Philosophy and Social Science Laboratory of Reading and Development in Children and Adolescents (South China Normal University), Ministry of Education Center for Studies of Psychological Application, South China Normal University, Guangzhou, China • <sup>2</sup>School of Psychology, South China Normal University, Guangzhou, China • <sup>3</sup>Department of Psychology and Behavioral Sciences, Zhejiang University, Hangzhou, Zhejiang, China • <sup>4</sup>Department of Experimental Psychology, University of Oxford, Oxford, United Kingdom • <sup>5</sup>Department of Neuropsychology, Institute of Cognitive Neuroscience, Faculty of Psychology, Ruhr University Bochum, Bochum, Germany • <sup>6</sup>State Key Laboratory of Cognitive Neuroscience and Learning & IDG/McGovern Institute for Brain Research, Beijing Normal University, Beijing, China • <sup>7</sup>Chinese Institute for Brain Research, Beijing, China • <sup>8</sup>School of Biomedical Engineering and Instrument Science, Zhejiang University, Hangzhou, China • <sup>9</sup>Qiushi Academy for Advanced Studies, Zhejiang University, Hangzhou, China • <sup>10</sup>Zhejiang Key Laboratory of Neurocognitive Development and Mental Health, Zhejiang University, Hangzhou, China

## eLife Assessment

This **important** study provides **solid** novel evidence for a role of ripples in the hippocampus in visual short-term memory. The work is strong in employing state-of-the-art intracranial electrophysiology in epilepsy patients with multivariate pattern classifiers in the context of an elegant experiment, but several aspects of the theoretical framing, mechanistic interpretation, and analysis strategy are **incomplete**.

<https://doi.org/10.7554/eLife.111304.1.sa3>

## Abstract

Emerging evidence suggests that hippocampus contributes to visual short-term memory (VSTM). However, the role of hippocampal ripple activity—brief high-frequency oscillations associated with memory replay—in supporting VSTM of naturalistic objects remains largely unknown. Here, using intracranial EEG recordings from human participants performing a delayed match-to-sample task, we found that hippocampal ripple rates progressively ramped up during the maintenance period and supported successful VSTM. More critically, hippocampal ripples were temporally coupled with the ripples in the lateral temporal lobe (LTL), and these coupled ripples were associated with the memory reactivation in the LTL. These findings provide direct evidence that hippocampal-neocortical interaction via coupled ripples supports VSTM, extending the hippocampal ripples' role to short-term mnemonic processes.

## Introduction

Early research suggested that the hippocampus is essential exclusively for long-term episodic memory formation<sup>1–3</sup>. However, emerging evidence implicates that the hippocampus also contributes to visual short-term memory (VSTM)<sup>4–7</sup>. For example, patients with focal hippocampal damage show impaired VSTM<sup>4,8,9</sup>. Moreover, item-specific VSTM representations could be decoded and reconstructed from the hippocampus<sup>10–12</sup>. These findings suggest that the hippocampus contributes to maintaining VSTM representations, yet the underlying mechanisms remain unclear.

The current study specifically focuses on the hippocampal ripple—a brief high-frequency oscillation (~80-150 Hz) that reflects synchronized activity of neuronal ensembles in the hippocampus<sup>13</sup>. Hippocampal ripple rates are initially well established in post-learning sleep, where learning increases ripple occurrence during subsequent slow-wave sleep<sup>14</sup>. In addition, enhanced hippocampal ripple rates have also been observed during successful memory encoding and long-term memory retrieval<sup>15–19</sup>. In contrast, their role in VSTM is far from clear. Recent rodent studies reported that selectively disrupting hippocampal ripples during awake learning impaired the working memory-dependent spatial navigation performance<sup>20,21</sup>, suggesting a possible—but still largely unexplored—contribution of ripples to VSTM.

The traditional persistent neural activity model of short-term memory suggests that memory is actively maintained through the sustained activation of neurons that selectively code memory content<sup>22</sup>. This view was originally inspired by early non-human primate studies<sup>23</sup> and further supported by some human iEEG studies showing persistently increased neural activity during delay periods in short-term memory tasks<sup>10,11</sup>. However, such persistent activity is not consistently observed in the neocortex, where the short-term memory information can be successfully decoded<sup>24,25</sup>. Moreover, hippocampal activity during maintenance is often at or below baseline for low memory loads, with increases under higher loads<sup>26</sup>. These findings motivated alternative dynamic coding models, which posit that VSTM representations are maintained not through sustained firing, but via short-term synaptic plasticity that stores information in an “activity-silent” hidden state<sup>27–30</sup>. According to these models, transient bursts are required to refresh the short-lived latent synaptic trace and thus maintain the stored representations. Moreover, these bursts are posited to “ramp up” toward the end of the retention interval, reflecting memory readout and preparation for responses<sup>30</sup>, a prediction supported by non-human primate research<sup>31,32</sup>.

Hippocampal ripples share key properties with these postulated reactivation bursts. They coordinate temporally compressed replay of neural firing patterns within the hippocampus<sup>13</sup> and are implicated in facilitating the transfer of these compressed hippocampal representations to distributed cortical networks during sleep-based memory consolidation<sup>33–36</sup>. Such hippocampal-neocortical coordination can be achieved via coupled ripple, i.e., co-occurrence of hippocampal ripples and neocortical ripples<sup>37</sup>, which have also been associated with successful memory retrieval<sup>18,38</sup>. In particular, we are interested in the interaction between the hippocampus and the lateral temporal lobe (LTL), a region implicated in representing memory-specific content during episodic memory retrieval<sup>18,39</sup>. These findings raise a key question: Do hippocampal ripples act as transient reactivation bursts that coordinate LTL activity to support human VSTM?

To answer this question, we analyzed iEEG recordings from the hippocampus (HPC) and lateral temporal lobe (LTL) in neurosurgical patients performing a VSTM task that required maintaining and then discriminating target images from highly similar lures. We found that hippocampal but not LTL ripple rates ramped up during the maintenance period, supporting VSTM accuracy. Critically, hippocampal ripples were temporally coupled with LTL ripples, and these coupled ripples further coincided with memory reactivation in the LTL. Importantly, these VSTM-related ripple dynamics cannot be attributed to formation of subsequent long-term memory. Together, these findings provide direct evidence that hippocampal ripples coordinate neocortical memory reactivation through dynamic coding mechanisms in supporting the VSTM.

## Results

### Behavioral results

Thirteen participants (mean age  $\pm$ SD: 26.77  $\pm$ 5.48 years, 7 females) with drug-resistant epilepsy were included in this study. The VSTM was assessed using a delayed match-to-sample (DMS) task comprising three stages: encoding, maintenance, and retrieval (Fig. 1a [↗](#), upper; see STAR Methods). In each trial, participants encoded a word-picture pair for 3 s. This was followed by a 7-second maintenance period, during which the picture was removed and participants were asked to vividly mentally maintain the picture. During the immediate retrieval stage, a probe picture—

either the original target or a highly similar lure—was presented, and participants indicated whether it matched the encoded picture (see Fig. 1a lower). All pictures were from four categories (i.e., animals, fruits, electrical devices, and furniture). Participants performed well in the DMS task with an accuracy of  $89.71 \pm 4.26\%$  (mean  $\pm$ SD) and a response time (RT) of  $1.03 \pm 0.22$  s (mean  $\pm$ SD). In addition, the RT for correct trials (i.e., remembered trials) was significantly shorter than that for incorrect trials (i.e., forgotten trials,  $t(12) = -5.88$ ,  $p < 0.001$ ). Note that the cue word in the DMS task was designed for a subsequent long-term memory cued-recall test, which enabled us to separate VSTM-related neural dynamics from those associated with long-term memory formation.

## Hippocampal ripple rates during the VSTM task

All participants were implanted with depth electrodes for clinical purposes. The iEEG data were recorded from the hippocampus during the DMS task (69 channels, mean  $\pm$ SD:  $5.31 \pm 5.01$  channels per patient; Fig. 1b). To investigate whether hippocampal ripples are modulated by VSTM, we first extracted ripples from individual hippocampal channels following the well-established protocols in the previous studies<sup>16,17,40</sup>. Specifically, raw iEEG data were bipolar re-referenced and filtered between 70 and 180 Hz (see STAR Methods). Then, the amplitude of the data was computed using a Hilbert transform, which was further rectified, squared, smoothed, and converted to z-scores. Ripple events were defined as transient amplitude fluctuations exceeding 4 SD above the pre-encoding baseline (i.e., 200-800 ms before stimulus onset), with durations in the range of 20 - 200 ms (Fig. 2a, see STAR Methods).

To validate our ripple detection procedures, we computed the ripple rate (i.e., number of ripple events per second) for individual hippocampal channels (see Fig. 2b upper panel for discrete ripples for individual trials from one exemplar channel). Across all task stages and participants, the mean ripple rate was 0.29 event/sec (Hz) (see Fig. S1), in line with previous studies<sup>16,17,40</sup>. Moreover, we replicated the novelty effect on ripple rates during memory encoding<sup>16</sup>. Specifically, hippocampal ripple rates were significantly higher for novel trials (i.e., the first presentation of VSTM items) than repeated trials (i.e., the second and third presentations of VSTM items) during encoding ( $p_{\text{cluster}} < 0.001$ , corrected by the non-parametric cluster-based permutation tests, see Fig. S2).

We next examined ripple rate change across different stages—encoding, maintenance, and retrieval. Hippocampal ripples occurred in 54.26% (SD = 13.55%) of trials during encoding, 78.74% (SD = 13.25%) during maintenance, and 26.85% (SD = 11.27%) during the pre-retrieval stage. Ripple rates were first averaged within each stage per trial. To account for trial-level variability, we then analyzed ripple rate changes across stages using a linear mixed-effects model with task stage as a fixed effect, with participant and trial as random effects (see STAR Methods). Our results showed that, compared to the pre-encoding baseline (i.e., -800 to -200 ms relative to stimulus onset), hippocampal ripple rates significantly increased during encoding and retrieval (all  $p_{\text{FDR}} < 0.009$ , multiple comparisons corrected by false discovery rate (FDR)) but not during maintenance ( $\beta = 0.141$ ,  $z = 2.462$ ,  $p_{\text{FDR}} = 0.079$ , Fig. 2c). Direct comparisons showed higher ripple rates during retrieval than during encoding ( $\beta = 0.042$ ,  $z = 7.203$ ,  $p_{\text{FDR}} < 0.001$ ) and maintenance ( $\beta = 0.046$ ,  $z = 8.018$ ,  $p_{\text{FDR}} < 0.001$ ), whereas encoding and maintenance did not differ significantly ( $\beta = 0.005$ ,  $z = 0.822$ ,  $p_{\text{FDR}} = 0.844$ ).

To further examine ripple dynamics at a finer time scale, we performed a time-resolved analysis by calculating the hippocampal ripple rates within consecutive 100 ms non-overlap sliding time windows for each task stage, averaging across channels for each participant. These ripple rates were then compared to the pre-encoding baseline across participants using cluster-based permutation tests<sup>41</sup>. The analysis revealed significant clusters showing increased hippocampal ripple rates during early encoding (0.15-0.85 s post stimulus-onset,  $p_{\text{cluster}} = 0.018$ ; Fig. 2b) and the late maintenance (7.85-8.15 s post stimulus-onset and 8.65-9.45 s post-stimulus onset,  $p_{\text{cluster}} < 0.034$ ). In contrast, ripple rates decreased significantly immediately after the response (0.05 s prior to 1.0 s post retrieval response,  $p_{\text{cluster}} = 0.001$ ), consistent with the decrease observed following long-term memory retrieval in previous studies<sup>17,40</sup>.

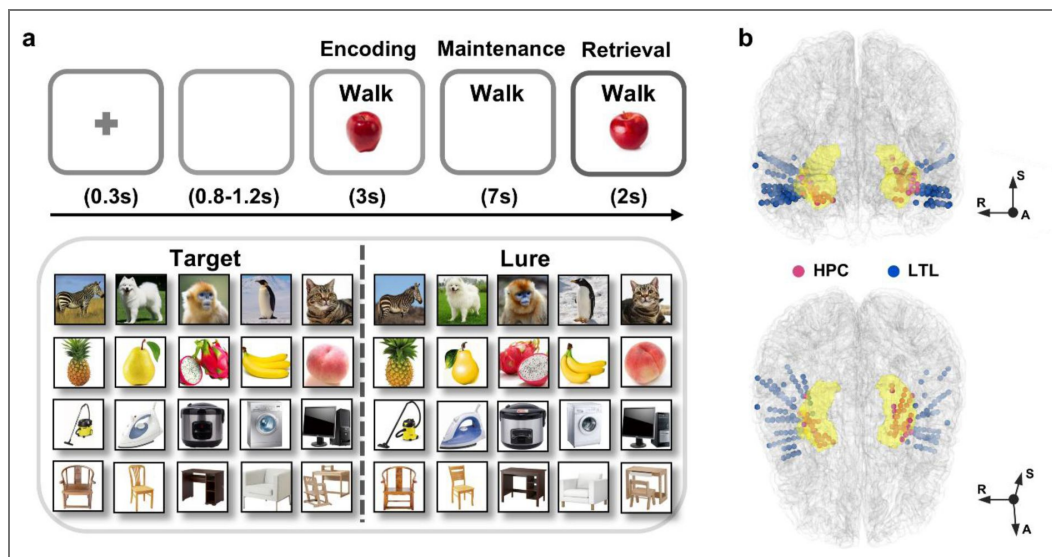


**Figure 1. Experimental paradigm, stimuli, and intracranial EEG channel localization.**

(a) Upper: an exemplar trial procedure of the delayed match-to-sample (DMS) task. Lower: examples of target and lure pictures. Pictures were selected from four categories—animals, fruits, electrical appliances, and furniture—with each row representing one category; (b) Normalized locations of intracranial EEG channels across all 13 participants. Pink spheres indicate hippocampal (HPC) channels within the highlighted yellow-shaded region, hippocampus; blue spheres indicate lateral temporal lobe (LTL) channels.

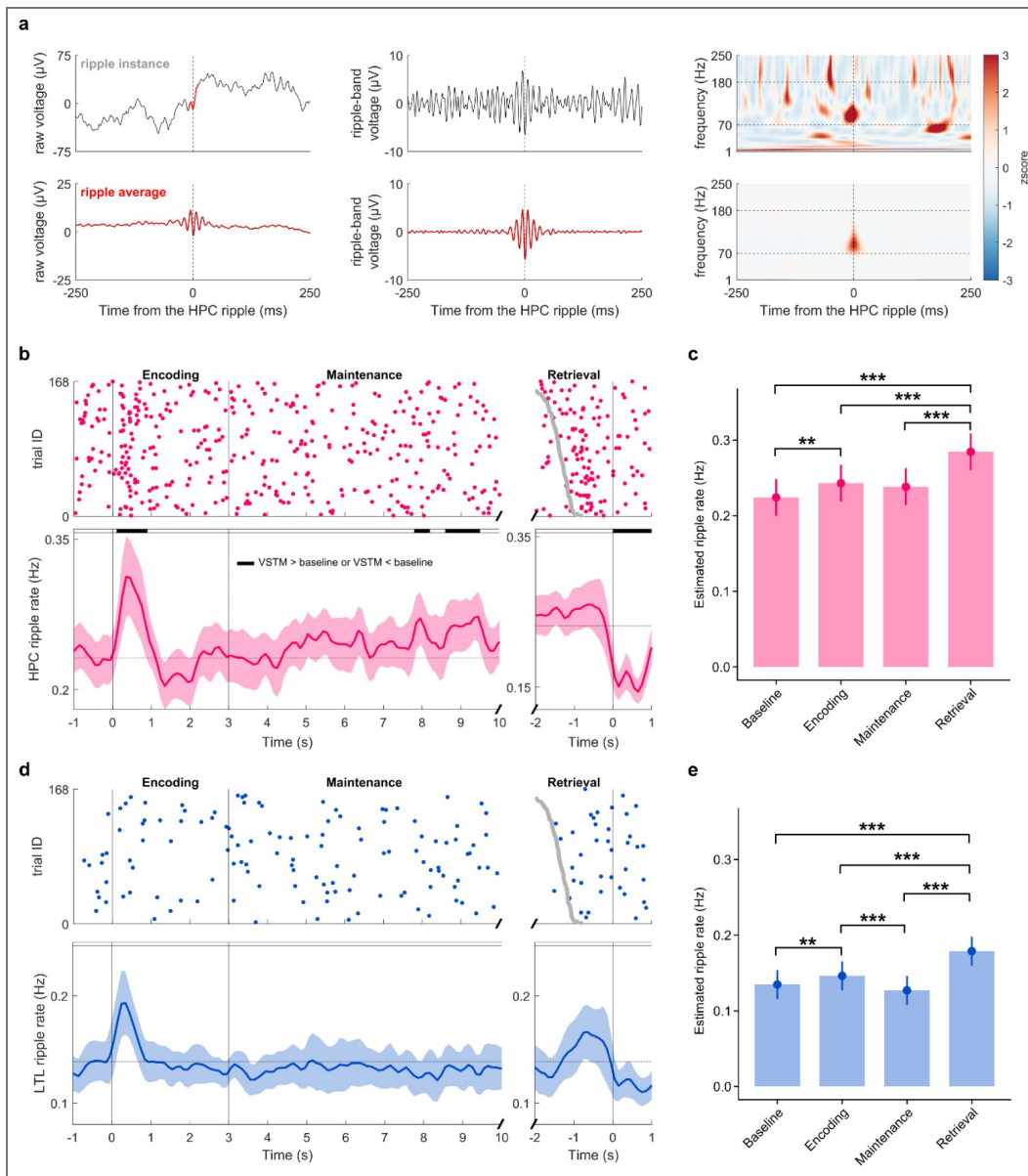


**Figure 2. VSTM task-induced ripple rate dynamics.**

**(a)** Examples of ripple activities from one hippocampal (HPC) channel. Upper (from left to right): a peri-ripple raw iEEG; ripple bandpass (70–180 Hz) filtered iEEG; Power spectrum of the peri-ripple iEEG. Lower (from left to right): averaged peri-ripple raw iEEG across ripples in a channel; averaged ripple bandpass filtered iEEG; averaged peri-ripple power spectrum; **(b)** Upper: Ripple raster plot for all individual trials from an example HPC channel. Trials are sorted according to reaction times. Each pink dot represents the peak time of a ripple. Lower: Time-resolved hippocampal ripple rates averaged across participants and channels during encoding, maintenance, and retrieval. The shaded areas around the lines indicate the standard error of the mean (SEM). The three vertical lines from left to right indicate onsets of encoding, maintenance, and retrieval response, respectively. The bolded grey curve represents the probe onset of each trial during retrieval; Black horizontal bars on the top of the lower panel indicate time clusters where ripple rates differ significantly from the pre-encoding baseline ( $p_{\text{cluster}} < 0.05$ ). **(c)** Linear mixed-effect model (LMM) estimated hippocampal ripple rates for pre-encoding baseline (0.2 to 0.8 s before stimulus) and individual task stages. Encoding: 0–3 s; maintenance: 3–10 s; retrieval: probe onset to response. **(d)** Upper: Ripple raster plot from an example LTL channel; Lower: Time-resolved LTL ripple rates averaged across participants and channels during encoding, maintenance, and retrieval. **(e)** LMM estimated LTL ripple rates for baseline and individual task stages. Black asterisks indicate significantly higher ripple rates relative to the pre-encoding baseline or significant differences between task stages. \*:  $p_{\text{FDR}} < 0.05$ , \*\*:  $p_{\text{FDR}} < 0.01$ , \*\*\*:  $p_{\text{FDR}} < 0.001$ , ns: not significant.

We next performed the same analyses on iEEG data from the lateral temporal lobe (LTL) in the same participants (132 channels; mean  $\pm$ SD: 10.15  $\pm$ 7.82 channels per patient; Fig. 1b). On average, LTL ripples occurred in 32.17% (SD = 14.69%) of trials during encoding, 52.34% (SD = 17.82%) during maintenance, and 14.99% (SD = 10.30%) during the pre-retrieval stage. Similar to the hippocampus, LTL ripple rates during encoding and retrieval were significantly higher than the pre-encoding baseline (both  $p_{\text{FDR}} < 0.002$ ), whereas maintenance did not differ from baseline ( $\beta = -0.008$ ,  $z = -2.505$ ,  $p_{\text{FDR}} = 0.059$ , Fig. 2d-e). Ripple rates during both encoding and retrieval were greater than during maintenance (both  $p_{\text{FDR}} < 0.001$ ), and retrieval showed higher ripple rates than encoding ( $\beta = 0.033$ ,  $z = 10.436$ ,  $p_{\text{FDR}} < 0.001$ ). The time-resolved group-level analysis revealed a significant cluster of increased ripple activity during early encoding (0.15-0.55 s post stimulus onset,  $p_{\text{cluster}} = 0.047$ ; Fig. 2d).

To assess whether hippocampal ripple rates were associated with VSTM performance, we first compared ripple rates between remembered and forgotten trials (i.e., memory accuracy), as well as between fast and slow responses among remembered trials (i.e., retrieval speed). Replicating previous studies<sup>17</sup>, hippocampal ripple rates are higher for successful than unsuccessful long-term memory retrieval (Fig. S2). However, no significant differences were observed between remembered and forgotten trials for any VSTM stages (all  $p_{\text{cluster}} > 0.466$ ; Fig. S2). Besides, fast and slow trials were defined as lower or higher than each participant's median reaction time (RT), respectively. Faster trials exhibited significantly higher ripple rates than slow trials during the pre-response retrieval ( $p_{\text{cluster}} = 0.014$ ; Fig. S2). Same analyses on LTL channels revealed no significant effects for either memory accuracy or retrieval speed ( $p_{\text{cluster}} > 0.237$ , Fig. S2).

These findings together suggest that while both hippocampal and LTL ripple rates were modulated by the VSTM task, these ripple rates were not associated with VSTM performance. Besides, for the hippocampal channels, ripple rates were above pre-encoding baseline during the late maintenance time windows, suggesting a potential ramping-up pattern that was tested in the following analyses.

## Ramping-up hippocampal ripples during maintenance supports successful VSTM

Next, we tested whether hippocampal ripples ramp up during the maintenance stage, as proposed by the dynamic coding framework<sup>30</sup>. Using a logistic generalized linear mixed-effects model (GLMM) with ripple occurrence as the dependent variable, maintenance time as fixed effects, and random intercepts/slopes for participants and trials, we observed a significant fixed effect of time across all trials ( $\beta = 0.012$ ,  $z = 4.678$ ,  $p < 0.001$ , Fig. S3), suggesting a ramping-up effect of hippocampal ripples. To examine whether this ramping-up predicted the VSTM performance, we further fitted a similar GLMM model with the interaction term: maintenance time  $\times$  VSTM accuracy (i.e., remember versus forget) as fixed effects (see STAR Methods). Our results revealed a significant interaction effect between VSTM accuracy and maintenance time ( $\beta = 0.018$ ,  $z = 2.171$ ,  $p = 0.030$ , Fig. 3a), indicating that the ripple ramping-up effects differed between remembered and forgotten trials. Post hoc analyses revealed a significant ramping-up for remembered trials ( $\beta = 0.014$ ,  $z = 5.024$ ,  $p_{\text{FDR}} < 0.001$ ), but not for the forgotten items ( $\beta = -0.002$ ,  $z = -0.282$ ,  $p_{\text{FDR}} = 0.778$ ).

Further control analyses revealed that the VSTM accuracy-related hippocampal ramping-up effect was robust across alternative ripple definitions (e.g., ripple duration  $\geq 25$  ms or alternative frequency bands: 80-120 Hz and thresholds following previous research<sup>18</sup>; see also STAR Methods and Fig. S3) and remained significant using conventional group-level analysis (STAR Methods and Fig. S3; see also Table S1 for participant-level ramping-up slopes). Moreover, the hippocampal ramping-up effect was unrelated to retrieval speed ( $\beta = 0.009$ ,  $z = 1.570$ ,  $p = 0.117$ ; Fig. S3) and did not differ between novel and repeated trials ( $\beta = -0.009$ ,  $z = -1.716$ ,  $p = 0.086$ ; Fig. S3).

We also tested the ripple ramping up during maintenance in the LTL. Unlike the hippocampus, no significant ramping-up was observed ( $\beta = -0.005$ ,  $z = -1.772$ ,  $p = 0.076$ , see Fig. S3), nor was the change in ripple rates over maintenance associated with VSTM accuracy (time  $\times$  accuracy

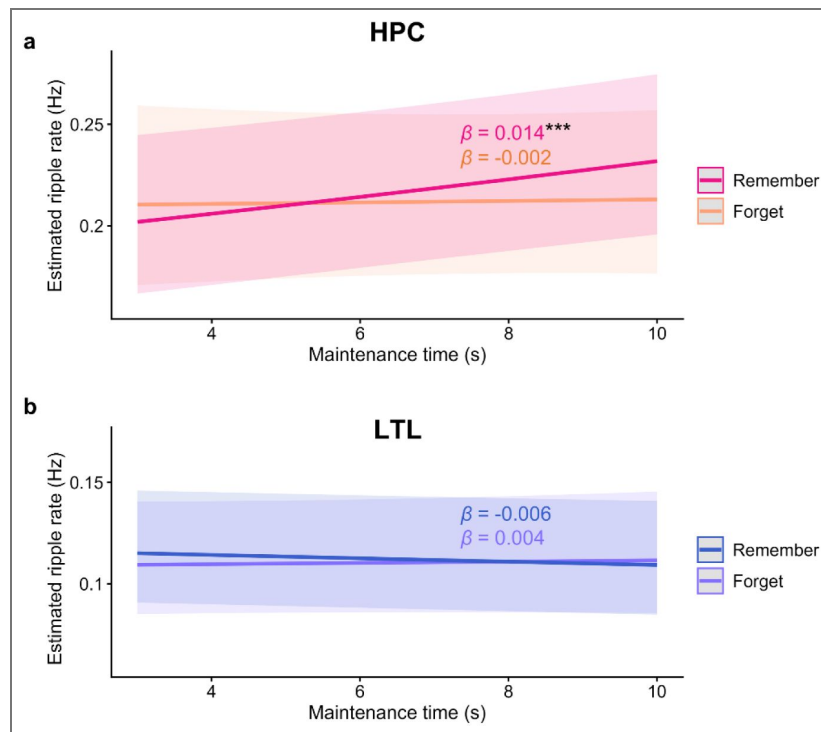


**Figure 3. Ripple ramping-up effects during maintenance.**

**(a)** Hippocampal (HPC) ripple ramping-up effects for remembered vs. forgotten trials. **(b)** Lateral temporal lobe (LTL) ripple ramping-up effects for remembered vs. forgotten trials. The shaded areas around the lines indicate the SEM.  $\beta$ : estimated fixed effect coefficients for remember or forget conditions.  $***: p_{FDR} < 0.001$ .

interaction effect:  $\beta = -0.010$ ,  $z = -1.246$ ,  $p = 0.213$ ; remember:  $\beta = -0.006$ ,  $z = -2.033$ ,  $p_{FDR} = 0.084$ ; forget:  $\beta = 0.004$ ,  $z = 0.507$ ,  $p_{FDR} = 0.612$ ; Fig. 3b [↗](#)) or RT (time  $\times$  RT interaction effect:  $\beta = 0.006$ ,  $z = 1.087$ ,  $p = 0.277$ , see also Fig. S3 [↗](#)). To ensure that the absence of a ramping-up effect was not due to low signal-to-noise channels, we restricted the analysis to 89 bipolar channel pairs with at least one contact in LTL gray matter or both contacts within 2 mm of it, and the results remained (see Fig. S3 [↗](#)). In addition, the absence of the ramping-up effect in the LTL cannot be attributed to greater signal heterogeneity compared with the hippocampus (see Fig. S3 [↗](#)).

## Hippocampal-LTL coupled ripples associate with VSTM performance

Previous research suggested that hippocampal ripples support memory via hippocampal-neocortical interactions<sup>35</sup>, which may be supported by ripple couplings across regions<sup>18,37,42</sup>. We therefore examined whether hippocampal-LTL ripple coupling supports VSTM. Following previous studies<sup>43,44</sup>, we computed the LTL ripple rate within  $\pm 0.5$  s of each hippocampal ripple peak (Fig. 4a [↗](#); See STAR Methods) across all task stages as well as within each task stage. For comparison, we computed LTL ripple rates within  $\pm 0.5$  s of randomly selected, hippocampal ripple-free time points for 1000 times, resulting in a surrogate distribution. The empirical coupled ripple rates were then z-scored against the surrogate distribution to yield a normalized coupled ripple index (see STAR Methods). Our results revealed that the normalized hippocampal-LTL coupled ripple index was significantly greater than zero across all task stages ( $p_{\text{cluster}} < 0.011$ ; Fig. 4b [↗](#)), and within individual stages (all  $ps_{\text{cluster}} < 0.047$ ).

To further investigate whether coupled ripples contribute to VSTM performance, we compared coupled ripple rates between remembered and forgotten trials. The results revealed significantly higher coupled ripple rates in remembered trials compared to forgotten trials during maintenance ( $ps_{\text{cluster}} < 0.019$ ; Fig. 4c [↗](#)). This effect remained significant after matching trial counts between remember and forget conditions using bootstrapping ( $ps < 0.040$ ). No significant differences were observed during encoding or retrieval stages ( $ps_{\text{cluster}} > 0.189$ ). Together, these findings suggest that hippocampal-LTL ripple coupling during the maintenance associated with successful VSTM.

## Hippocampal-LTL coupled ripples coordinate memory reactivation in the LTL

We next tested whether hippocampal-LTL coupled ripples support the VSTM reactivation in the LTL. To this end, we applied a multivariate decoding method to the spectral power of LTL channels for individual participants to classify categories of learned pictures (see STAR Methods). Classifiers were trained on each encoding time window and tested across encoding, maintenance, and retrieval time windows. Among remembered trials, we identified significant clusters showing decoding accuracies above chance level (25%) during encoding, early maintenance, and retrieval (all  $ps_{\text{cluster}} < 0.039$ , Fig. 5a [↗](#)). When averaged across all time windows within each stage, decoding accuracy remained significantly above chance for individual stages (all  $ps_{FDR} < 0.003$ , Fig. 5b [↗](#)). Note that the above-chance decoding during the maintenance stage cannot be simply attributed to the lingering sensory input immediately following encoding. This effect remains robust in the 3–4 s post-encoding interval (Fig. S4 [↗](#)). Furthermore, remembered items showed greater decoding accuracy than forgotten ones during the pre-response retrieval stage (Fig. S4 [↗](#)). These results suggested that VSTM is represented and reactivated in the LTL.

We then tested whether this reactivation was temporally locked to the hippocampal-LTL coupled ripples during remembered trials. To enhance signal-to-noise ratio, we pooled hippocampal-LTL coupled ripples across all task stages (mean  $\pm$ SD: 439  $\pm$ 125 coupled ripples per participant) and aligned decoding accuracy to  $\pm 0.5$  s around hippocampal ripple peaks of the LTL coupled ripples. Notably, the decoding accuracy was z-scored relative to the surrogate distribution, where decoding accuracy aligned to non-coupled ripple time points, and then tested against zero (see STAR Methods). Our results revealed a significant positive cluster when the classifier was trained on late encoding windows (1.85–2.25 s post-stimulus;  $p_{\text{cluster}} = 0.029$ ; Fig. 5c [↗](#)), indicating LTL memory

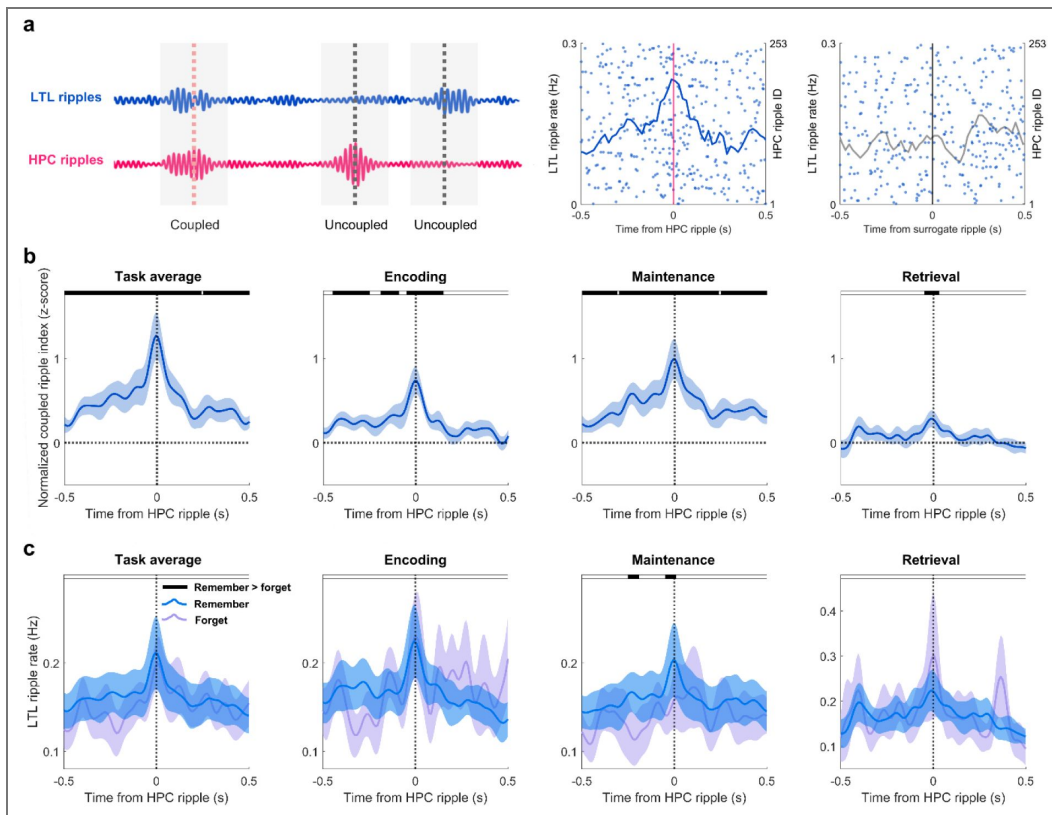


**Figure 4. Hippocampal-LTL coupled ripples.**

(a) Left: Illustration of coupled ripples between HPC and LTL (first shaded area) and uncoupled HPC ripple (second shaded area) and LTL ripple (third shaded area). Middle: LTL ripple rates time-locked to an exemplar HPC ripple from one participant; Right: LTL ripple rates time-locked to surrogate time points without HPC ripples from the same channels. Each row indicates LTL ripples locked to a single HPC ripple peak or surrogate time point. Each blue dot represents an LTL ripple, and the curve shows LTL ripple rates across all trials surrounding HPC ripple peaks or surrogate time points. (b) Normalized hippocampal-LTL coupled ripple index across all task stages (i.e., task average) and within individual task stages. (c) Hippocampal-LTL coupled ripple rate difference in remembered versus forgotten trials. Black bars at the top indicate time windows with significant differences between conditions (survived after cluster-based permutation tests:  $p_{\text{cluster}} < 0.05$ ). The shaded areas around the lines indicate the SEM.

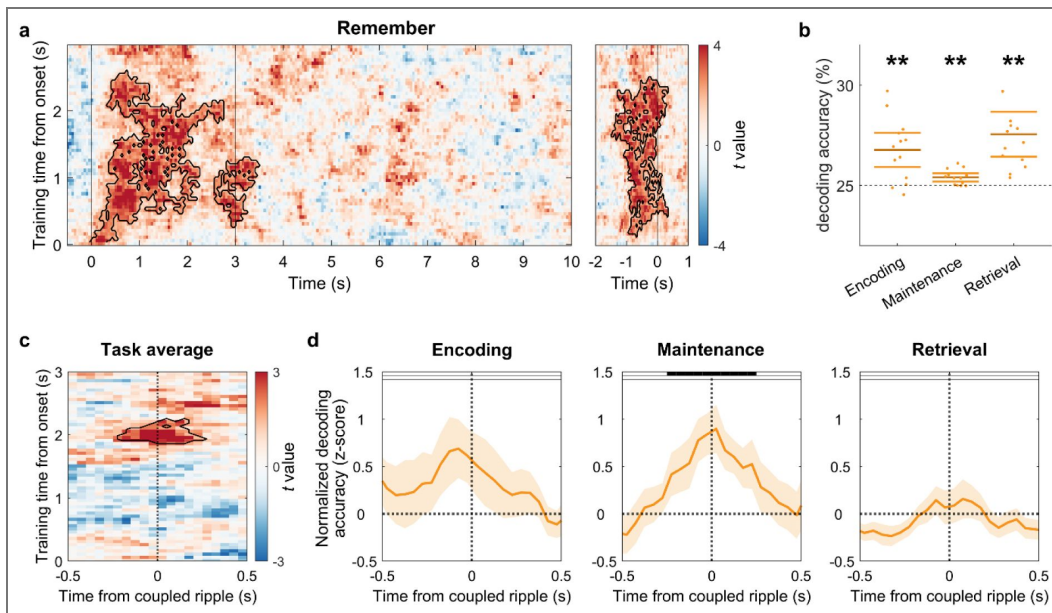


**Figure 5. Coupled ripples coordinate memory reactivation in the LTL.**

**(a)** LTL decoding accuracy of remembered trials compared to chance level (25%) across the task (left: encoding and maintenance, 0 indicates stimulus onset; right: retrieval, 0 indicates behavior response). Clusters with significantly above-chance decoding accuracy (survived cluster-based permutation test) are circled by black lines. **(b)** Decoding accuracies during encoding, maintenance, and retrieval stages are significantly above chance. **(c)** Normalized decoding accuracy time-locked to hippocampal-LTL coupled ripples relative to surrogate distribution. The black-circled cluster indicates normalized decoding accuracy significantly above zero. **(d)** Coupled ripple-locked normalized decoding accuracy averaged across the late encoding cluster identified in (c). Black bars at the top indicate significant clusters with normalized decoding accuracy significantly above zero. All clusters survived cluster-based permutation tests ( $p_{\text{cluster}} < 0.05$ ). The shaded areas around the lines indicate the SEM. \*\*:  $p_{\text{FDR}} < 0.01$ .

reactivation time-locked to coupled ripples. Further analysis based on the identified cluster, we found that this coupled ripple-locked decoding accuracy was significant during maintenance ( $p_{\text{cluster}} = 0.004$ , Fig. 5d), but not during the encoding or retrieval stage ( $p_{\text{cluster}} > 0.118$ ). Notably, coupled ripple-locked LTL decoding accuracy in the clusters in Fig. 5c and 5d was significantly above chance (i.e., 25%; all  $p_s < 0.002$ ).

As a control analysis, we also examined memory reactivation in the hippocampus and its temporal link with hippocampal-LTL coupled ripples. Although hippocampal decoding accuracy was above chance when averaged across time windows for each task stage ( $p_{\text{FDR}} < 0.031$ ), it was not significantly time-locked to hippocampal-LTL coupled ripples ( $p_{\text{cluster}} > 0.470$ ; Fig. S5). Further control analyses to test the specificity of coupled ripple revealed that decoding accuracy in neither the hippocampus nor the LTL was modulated by independent, uncoupled ripples (i.e., hippocampus or LTL ripples without coupling) ( $p_{\text{cluster}} > 0.203$ ; Fig. S5). These findings suggest that coupled hippocampal-LTL ripples coordinate memory reactivation in the LTL, rather than in the hippocampus, during VSTM maintenance.

## VSTM-related ripple dynamics are not associated with subsequent long-term memory performance

To rule out potential confounds from long-term memory (LTM) formation, we separated VSTM-remembered trials based on whether they were later remembered or forgotten in the LTM test and compared the hippocampal ramping-up effect, hippocampal-LTL coupled ripples, and coupled ripple-locked memory reactivation between these two conditions. Our results showed that the hippocampal ripple ramping-up effect was significant for both subsequently LTM remembered ( $\beta = 0.017$ ,  $z = 4.141$ ,  $p_{\text{FDR}} < 0.001$ ) and forgotten trials ( $\beta = 0.011$ ,  $z = 2.987$ ,  $p_{\text{FDR}} = 0.003$ ; see Fig. S6). Critically, no significant difference was observed between subsequently LTM remembered and forgotten items ( $\beta = 0.003$ ,  $z = 0.439$ ,  $p = 0.661$ ). Moreover, neither the coupled ripple rate nor ripple-locked reactivation differed between subsequently LTM remembered and forgotten trials (Fig. S6). Together, these control analyses suggest that our main findings reflect mechanisms underlying VSTM rather than LTM.

## Discussion

While previous rodent and recent human studies have implicated hippocampal ripples in long-term memory consolidation and retrieval<sup>16,45</sup>, it remains unclear whether and how hippocampal ripples support human VSTM. Our study provides novel electrophysiological evidence that hippocampal ripples and their coordination with the neocortex support VSTM. We found that hippocampal ripples progressively ramped up during the maintenance period, and this ramping-up effect was associated with successful VSTM. Moreover, hippocampal ripples were temporally coupled with LTL ripples, and these coupled events coincided with memory reactivation in the LTL during maintenance.

First of all, no overall above-baseline hippocampal ripple rate when averaged across the 7-s maintenance time windows, combined with the above-baseline ripple rates during late maintenance and the ripple ramping-up effect over the 7-s maintenance period, collectively aligns with the dynamic coding framework of VSTM<sup>30</sup>. The ramping-up in hippocampal ripple rates is associated with memory accuracy but not reaction time, suggesting its role in proactive memory retrieval during VSTM rather than general arousal or motor preparation<sup>46,47</sup>. Moreover, this ramping-up effect is unlikely to reflect signal drifts over long intervals, since it was observed exclusively in remembered trials and has also been reported in studies using shorter retention periods, such as 1.5 s<sup>48</sup> or 3 s<sup>49</sup>. Nonetheless, we cannot rule out the possibility that the magnitude of this effect may be affected by the duration of the delay period. Future studies could systematically manipulate retention intervals to test this possibility. In addition, we found hippocampal ripple rates decreased immediately following the response, a pattern consistent with that during episodic memory retrieval<sup>17,40</sup>, which may reflect diminished hippocampal engagement following memory retrieval.

While our findings align with the dynamic coding framework of VSTM, they appear to contrast with prior reports of persistent hippocampal spiking during short-term memory maintenance<sup>10,11</sup>. Several factors may account for this discrepancy, including differences in neural measures, task demands. First, prior studies identifying persistent activity were mostly based on single-unit recordings<sup>10,11,23</sup>, revealing sustained firing in a minority of stimulus-selective neurons. In contrast, our local field potential (LFP) recordings may reflect a dynamic coding scheme at the population level<sup>30</sup>. Compared to persistent firing, this dynamic population coding is less constrained by memory capacity limits and may offer more flexible control while minimizing inter-item competition<sup>50</sup>. Second, contemporary short-term memory models suggest that items within the focus of attention are maintained via persistent activity, while unattended items are stored in an activity-silent state<sup>51,52</sup>. Therefore, multi-item VSTM tasks with higher attentional demands may favor persistent activity, while our single-item task may have allowed memory to drift out of focus, favoring an overall activity-silent state with discrete reactivation bursts. Corroborating this possibility, a previous study found persistently increased hippocampal gamma band activity during multi-item working memory maintenance but not for the single-item<sup>26</sup>.

Critically, our findings suggest that hippocampal ripples serve as high-frequency bursts that coordinate memory representational refresh during the short-term memory maintenance period. While these ripples are sparse in time, they fit the proposed functional role of high-frequency bursts that intermittently refresh synaptic weights, thereby maintaining the learning-induced, short-lived changes<sup>28–30</sup>. Corroborating our finding, recent rodent research shows that hippocampal activity during VSTM delays is characterized by low-rate activity that supports memory reactivation<sup>53</sup>. Complementing these studies, we show that hippocampal ripples coordinate memory reactivation through coupling with LTL ripples, suggesting that hippocampal ripples refresh memory traces not only in the hippocampus but also in the neocortex. Together with the previous human intracranial studies of hippocampal ripples during episodic memory<sup>16,17,40</sup>, these findings convergently support the functional significance of low-rate hippocampal activity.

In addition, we emphasize that hippocampal ripples are unlikely to be the sole mechanism supporting VSTM. For example, prior work has shown that gamma bursts in the prefrontal cortex gate access to encoded VSTM representations and that ramping of such bursts supports working memory in primates<sup>48</sup>. Moreover, recent rodent research demonstrates that replay sequences can occur even in the absence of sharp-wave ripples<sup>54</sup>. These findings suggest that ripple ramping-up should be interpreted as one component within a broader, distributed set of dynamic mechanisms supporting short-term memory maintenance. However, the use of iEEG in humans limited us from direct observation of full brain network, and future studies combining broader spatial coverage with high temporal resolution will be essential for characterizing how hippocampal ripples interact with complementary maintenance mechanisms.

Notably, our findings show that memory reactivation was locked to coupled ripples in the hippocampus and LTL, rather than isolated ripples in either the hippocampus or the LTL, highlighting the necessity of hippocampal-neocortical communication. Our work further demonstrated that coupling strength was associated with VSTM accuracy, which is consistent with prior findings showing that increased hippocampal-neocortical functional connectivity, from pre- to post-encoding rest, is associated with subsequent memory performance<sup>55</sup>. Comparing with previous research emphasizing low-frequency coordination supporting VSTM—such as theta-band (4–5 Hz) phase coherence between hippocampus and neocortex<sup>56</sup> and 1–10 Hz oscillations modulating memory reactivation<sup>57</sup>, our findings suggest hippocampal-cortical communication could be achieved through an alternative mechanism: the co-occurrence of ripples. Consistent with our findings, the latest evidence shows that ripples in different brain areas co-occur with near-zero phase lag, providing a temporally precise mechanism for efficient inter-regional communication<sup>42</sup>. These different neural mechanisms—low-frequency coherence and ripple co-occurrence—may not necessarily be mutually exclusive. One possibility is that hippocampal ripples are nested within ongoing theta oscillations during cross-regional communication<sup>58</sup>, a hypothesis that remains to be tested in future research.

We acknowledge that the use of familiar, semantically rich everyday objects in our delayed match-to-sample task likely engages long-term memory (LTM) processes. Prior work suggested that short-term performance can be supported by pre-existing semantic knowledge and episodic experience, such that hippocampal engagement may reflect interactions between visual perceptual input and long-term pre-existing knowledge/episodes, rather than a strictly process-pure visual short-term memory (VSTM)<sup>59–61</sup>. Although prior work has often used abstract stimuli to minimize episodic contributions<sup>62</sup>, disentangling VSTM from LTM was not the primary aim of this study. Moreover, recent evidence suggests that simplified stimuli may underestimate how the brain maintains meaningful information in real-world contexts<sup>61</sup>. Indeed, semantically rich stimuli can enhance working memory capacity by enabling access to long-term representations<sup>63–66</sup>. We therefore interpret our findings as reflecting mechanisms that support the short-term maintenance of meaningful, real-world visual representations. Future studies aiming to more strictly dissociate VSTM from LTM contributions should employ artificial or abstract stimuli that minimize pre-existing knowledge associations.

Moreover, our findings showed that both the ramping-up hippocampal ripple rates and the hippocampal-LTL coupled ripples during maintenance were associated with VSTM rather than subsequent LTM accuracy. These findings suggest that the ripple dynamics we observed primarily support the short-term maintenance of complex visual features and their binding within the pictures themselves rather than the formation of long-term memory for cue-picture pairs, which has been shown in previous research<sup>39</sup>. This interpretation is strengthened by recent studies showing that hippocampal ripples and hippocampal neuronal firing support VSTM of complex naturalistic pictures in the absence of subsequent LTM tests or cue-picture associations<sup>67,68</sup>. Moreover, converging evidence from studies on neural oscillations, patients with focal hippocampal damage, and neural modulation demonstrates that the hippocampus plays a critical role in VSTM, where high-resolution feature binding is required<sup>4,8,9</sup>.

Beyond binding demands, the hippocampus also contributes to VSTM for simple visual features that minimally engage LTM, such as color squares, when memory precision is dissociated from binding errors or when relational demands are minimized<sup>4,69</sup>. For instance, previous research found that patients with hippocampal damage exhibited reduced precision for simple color memories after brief delays, yet showed no increase in relational binding errors<sup>4</sup>. Similarly, a recent study demonstrated that MTL lesions selectively impair the precision of VSTM representations rather than the quantity of items retained<sup>69</sup>. In addition, the hippocampus is also known to engage in tasks with relatively low memory precision demands, such as change detection paradigms requiring only coarse-level discrimination between targets and distinct lures<sup>6,10,67</sup>. These findings collectively indicate that the hippocampus supports a wide range of VSTM tasks. Future work should systematically examine whether key factors, such as relational binding demands and memory precision, shape hippocampal ripple dynamics, using experimental manipulations or multi-component modeling<sup>70</sup>.

The absence of differences in ripple rates and category-level decoding accuracy between VSTM remembered and forgotten trials during maintenance may reflect that hippocampal ripples serve dual functions. While they support high-fidelity memory reactivation to discriminate the highly similar lures from target pictures in remembered trials, they may also coordinate coarser, less precise reactivation for forgotten trials. These coarse representations are likely insufficient and less accessible to support fine discrimination. Supporting this interpretation, we observed that memory decoding evidence was lower for forgotten items compared with remembered items prior to VSTM retrieval responses.

In addition, the ripple ramping-up effect was only observed in the hippocampus but not in the LTL, despite the well-documented role of LTL in representing VSTM content<sup>39,71</sup>. The absence of LTL ripple ramping-up cannot be attributed to more heterogeneous ripple activity in LTL channels. However, our LTL coverage spanned inferior, middle, and superior temporal lobes, due to the patients' clinical implantation scheme, which prevented us from restricting analyses to specific subregions. Consequently, we cannot rule out the possibility that ramping-up effects may exist in more restricted LTL subregions. In addition, our results raise an important question of

whether similar ripple ramping-up effects occur in other brain regions. Future studies with broader and more targeted electrode coverage, including prefrontal and occipital cortices known to interact with the hippocampus during VSTM, will be necessary to address these questions<sup>72,73</sup>.

To conclude, our study provides direct electrophysiological evidence that hippocampal ripples—and their coordination with neocortical regions—support VSTM. We show that ripple activity in the hippocampus ramps up during maintenance and is associated with memory accuracy. These findings support a dynamic coding model of VSTM and suggest that hippocampal ripples orchestrate discrete reactivations that sustain latent representations. By linking ripple dynamics to both representational reactivation and interregional coupling, our results extend the hippocampus's role from long-term formation to short-term memory maintenance and offer new insights into the neural mechanisms unifying these memory systems.

## STAR★Methods

### Resource availability

#### Lead contact

Further information and requests for resources should be directed to and will be fulfilled by the lead contact: Ying Cai ([yingcai@zju.edu.cn](mailto:yingcai@zju.edu.cn) [✉](#)).

#### Materials availability

This study did not generate new unique reagents.

### Experimental model and study participant details

#### Participants

We reanalyzed the data from a previous study<sup>57</sup>. We included thirteen epilepsy patients (mean age  $\pm$ SD: 26.77  $\pm$ 5.48 years, 7 females) who had electrodes implanted in both the hippocampus and LTL. The iEEG data were recorded at the Center of Epileptology, Xuanwu Hospital, Capital Medical University, Beijing, China. The study adhered to the latest version of the Declaration of Helsinki and was approved by the Institutional Review Board at Xuanwu Hospital. All participants have a normal or corrected-to-normal visual acuity. They all signed written informed consent before the experiment.

#### Method details

##### Stimuli and procedures

The study consisted of a visual short-term memory (VSTM) task, followed by a 1-minute countback task and a short break (1 to 4 minutes), and then a cued-recall long-term memory test. The study used 56 pictures of familiar everyday objects and 112 two-character Chinese verbs. The pictures were drawn from four categories—fruits, animals, electrical devices, and furniture—with 14 images per category. Each picture was randomly paired with two different cue words across two consecutive experimental runs.

The VSTM was assessed using a modified Delayed Match-to-Sample (DMS) task. In each run, participants studied 14 unique word-picture pairs, each repeated three times, resulting in 42 trials per run. Each trial started with a brief fixation period (300 ms), followed by a jittered blank interval (800-1200 ms). A cue word and its associated target picture were then presented centrally for 3 s, during which participants were instructed to encode the association between the word and the picture. Immediately following the encoding stage, the picture disappeared while the cue word remained on screen for 7 s. During this maintenance stage, participants were instructed to mentally maintain a vivid image of the target picture. Displaying the cue word during maintenance served to reinforce the word-picture association, reduce working memory load, and minimize distraction. It was then followed by an immediate retrieval stage, during which a probe picture was displayed on the screen, and participants were instructed to determine whether it matched the target picture by pressing one of two buttons within 2 s. The probe picture was either

REAGENT or RESOURCE	SOURCE	IDENTIFIER
<b>Deposited data</b>		
Dataset used in the present study	N/A	<a href="https://osf.io/gwe62/?view_only=39b3ddbcaae342c8a2696a1e16473712">https://osf.io/gwe62/?view_only=39b3ddbcaae342c8a2696a1e16473712</a>
<b>Software and Algorithms</b>		
Matlab R2022b	RRID: SCR_001622	<a href="http://www.mathworks.com/products/matlab/">http://www.mathworks.com/products/matlab/</a>
EEGLAB (v2021.1)	RRID:SCR_007292	<a href="http://scn.ucsd.edu/eeglab/index.html">http://scn.ucsd.edu/eeglab/index.html</a>
FieldTrip (v20240731)	RRID:SCR_004849	<a href="https://www.fieldtriptoolbox.org">https://www.fieldtriptoolbox.org</a>
RStudio (v2025.09.01)	RRID:SCR_000432	<a href="https://posit.co/">https://posit.co/</a>
R (v4.5.1)	RRID:SCR_001905	<a href="https://www.r-project.org/">https://www.r-project.org/</a>
R-package lme4 (v1.1.37)	RRID:SCR_015654	<a href="https://cran.r-project.org/web/packages/lme4/index.html">https://cran.r-project.org/web/packages/lme4/index.html</a>
R-package lmerTest (v3.1.3)	RRID:SCR_015656	<a href="http://CRAN.R-project.org/package=lmerTest">http://CRAN.R-project.org/package=lmerTest</a>

**Key resources table.**

the same as the target picture (50%, match trials) or a highly similar lure picture (50%, nonmatch trials). Each participant completed between 4 and 8 DMS runs (mean  $\pm$ SD: 6.14  $\pm$ 1.46), resulting in a total of 168-336 trials (mean  $\pm$ SD: 258.00  $\pm$ 61.32) per participant.

In the cued-recall long-term memory test, a cue word was presented on screen, and participants reported the category of the associated picture by pressing one of four buttons corresponding to the four object categories. The current study focused primarily on VSTM stages, with the cued-recall data included as a control to help dissociate VSTM-related processes from long-term memory.

## Quantification and statistical analysis

### Data recordings and preprocessing

Intracranial EEG data were recorded from depth electrodes, each containing 12 or 16 channels (2 mm in length, 0.8 mm in diameter, spaced 1.5 mm apart). Data were collected using amplifiers from Brain Products (Brain Products GmbH), NeuroScan (Compumedics Limited), or Nicolet (Alliance Biomedica Pvt Ltd.) electroencephalogram systems, with the sampling rates of 2,500, 2,000, and 2,048 Hz, respectively. During the online recordings, data from all channels were referenced to a common subcutaneous channel. During the offline preprocessing, we first removed the channels within the epileptic loci and channels that were severely contaminated by epileptic activity. The remaining channels in the hippocampus (HPC) and lateral temporal lobe (LTL) were visually inspected and bipolar referenced to channels on the same electrode. Because not all participants had multiple hippocampal channels on the same electrode, HPC channels were bipolar re-referenced to the nearest white matter channel<sup>40,74</sup>. LTL channels were bipolar re-referenced to an adjacent channel within the LTL<sup>39</sup>.

### Channel localization

The identification of channel locations included the following steps. First, each participant's post-implantation CT scan was co-registered with their pre-implantation MRI. The MRI was then normalized to Montreal Neurological Institute (MNI) space using Statistical Parametric Mapping 12 (SPM12). Anatomical localization and 3D visualization of electrode channels were conducted using the 3D Slicer platform (<https://www.slicer.org/>). To assign anatomical labels, structural MRIs were segmented with FreeSurfer (<https://surfer.nmr.mgh.harvard.edu>), and the nearest cortical or subcortical label was assigned to each channel. Channels in the hippocampus were further verified through visual inspection in each participant's native anatomical space.

### Ripple detection and peri-ripple spectral analysis

Ripple detection followed the established procedures outlined in previous studies<sup>16,17,40</sup>. First, a 70-180 Hz bandpass linear-phase Hamming-windowed finite impulse response (FIR) filter was applied to the bipolar re-referenced iEEG data on HPC and LTL channels, with a transition width of 5 Hz. We then computed the analytic signal amplitude (squared) using the Hilbert transform. To determine the ripple detection threshold, we: (1) identified and clipped extreme values ( $\geq 4$  SD above mean) using the Least-Median-Square (LMS) method to reduce outlier bias; (2) smoothed the clipped signal with a 40 Hz low-pass Kaiser-windowed FIR filter (5 Hz transition); (3) calculated the mean and SD of ripple-band amplitude across all runs per channel. Candidate ripples were defined as periods when the squared amplitude exceeded 4 SD above the mean, with start/end points marked by crossings of 2 SD. Events lasting  $< 20$  ms or  $> 200$  ms were excluded. Ripple peaks were identified with MATLAB's findpeaks.m, and events with  $< 30$  ms peak-to-peak intervals were merged.

To validate the results from the above ripple detection approach, we have also performed an alternative ripple detection method following previous research<sup>18</sup>. Specifically, we first bandpass-filtered the iEEG signal in the ripple range (80-120 Hz) using a second-order Butterworth filter and then applied a Hilbert transform to extract the instantaneous amplitude. Candidate events were identified when the Hilbert envelope exceeded 2 SD above the mean amplitude. Events were kept as ripples only if they lasted at least 25 ms and reached a peak amplitude >3 SD. Adjacent events separated by <15 ms were merged.

To prevent contamination from pathological activity, interictal epileptiform discharges (IEDs) were rigorously screened. Channels within clinically identified epileptogenic zones were excluded. For the remaining channels, IEDs were independently verified by two neurologists at Beijing Xuanwu Hospital. IEDs typically exhibit broadband power increases (1-180 Hz), whereas physiological ripples show narrow high-frequency activity (70-180 Hz). Candidate ripple events exhibiting broadband spectral increases or occurring within 50 ms of an IED were excluded.

To obtain the peri-ripple spectrograms, we first epoched iEEG data into 6-s segments, ranging from 3 s before the ripple peak to 3 s after it. The epoched data were then convolved with complex Morlet wavelets (six cycles) in the range of 1 to 250 Hz, with 2 Hz steps. The resulting complex wavelet transform was squared to obtain spectral power. Power values were z-transformed for each frequency and channel using the mean and the SD of the power across all epochs belonging to the same experimental run. Final spectrograms were centered around ripple peaks ( $\pm 250$  ms) in 500-ms windows. All iEEG analyses were performed in MATLAB using custom scripts and functions from the FieldTrip toolbox<sup>75</sup>.

### Analysis of ripple rate changes and cluster-based permutation test

Detected ripples were time-locked to stimulus onset for the encoding and maintenance stages, and to behavioral responses for the retrieval stage. For each trial, ripple rate was calculated by dividing the number of ripples by the duration (in seconds) of each task stage: encoding (0-3 s post-stimulus onset), maintenance (3-10 s), and retrieval (from probe onset to response). The ripple rate in a pre-encoding time window (200 to 800 ms prior to stimulus onset) was also computed and served as the baseline.

We used linear mixed-effect model (LMM) analysis to compare the ripple rates between each VSTM task stage and the pre-encoding baseline, as well as between different task stages. The analysis was performed using the R package lme4<sup>76</sup>. The models were specified as follows:

$$\text{ripple\_rate} \sim \text{stages} + (1 \mid \text{participant}) + (1 \mid \text{participant} : \text{trial})$$

Here, *ripple\_rate* refers to the ripple rate per channel, and *stages* is a fixed effect with four levels: pre-encoding baseline, encoding, maintenance, and retrieval. Random intercepts were included for each participant and for trials nested within participants to account for within-subject and within-trial variability. Pairwise comparisons between stages were performed using the emmeans package, and the resulting *p*-values were corrected for multiple comparisons using the Benjamini-Hochberg false discovery rate (FDR) procedure<sup>77</sup>.

To quantify ripple rate changes at a finer temporal resolution, we computed ripple rates using non-overlapping 100-ms time windows within each task stage. The resulting time series was smoothed using a 400-ms Gaussian kernel. Ripple rates were then compared to the pre-encoding baseline separately for the encoding, maintenance, and retrieval stages. To correct for multiple comparisons, we performed non-parametric cluster-based permutation tests using the MATLAB codes (<https://doi.org/10.5281/zenodo.10877825>). Specifically, for each time point, we computed the empirical ripple rate difference between conditions (e.g., encoding vs. baseline). We then compare it to a null distribution of ripple rate differences, which were generated by randomly permuted condition labels (e.g., encoding vs. baseline) 5,000 times. At each iteration, the ripple rate difference between conditions was recalculated. The empirical threshold for significance ( $\alpha = 0.05$ , two-tailed) was determined from this null distribution. Time points of empirical ripple rate difference exceeding this threshold were grouped into clusters. For each cluster, a cluster-level

statistic was computed by summing the ripple rate differences within the cluster. The observed cluster statistics were then compared against the distribution of maximum and minimum cluster-level statistics derived from the 5,000 permutations to determine significance. This same cluster-based permutation procedure was also used to compare ripple rates between remembered and forgotten trials, and between fast and slow remembered trials.

### Ramping-up effects analysis

To test whether the ramping-up of ripple activity during maintenance predicted VSTM performance, we fit generalized linear mixed-effects models (GLMMs) with a Poisson link function. The main model was specified as:

$$\text{ripple} \sim 1 + \text{time} \times \text{memory} + (1 + \text{time} \mid \text{participant}) + (1 + \text{participant} \mid \text{trial})$$

Here, *ripple* refers to the trial-level ripple count (Poisson-distributed). *Time* corresponds to the 7-s maintenance time index, and *memory* reflects VSTM accuracy (remembered = 1, forgotten = 0) or response speed (fast vs. slow), entered as fixed factors. Random intercepts and time slopes were included for each participant, and random intercepts for trials nested within participants. When this time  $\times$  memory interaction effect was significant, we conducted follow-up analyses by fitting separate GLMMs for remembered and forgotten trials (or fast and slow trials). These post-hoc models tested whether ripple activity increased over time within each memory outcome, and corresponding *p*-values were further FDR corrected.

To validate our GLMM results, we also performed a group-level ramping-up analysis. Ripple rates were first averaged across trials and channels, yielding a time series of mean ripple rates during the maintenance stage for each participant. A linear regression was then applied to each participant's ripple rate time series, with the regression slope quantifying the change in ripple rates over time. Independent *t*-tests were used to assess whether slopes were significantly greater than zero for remembered and forgotten trials, and to compare slopes between these two conditions.

### Coupled ripple analysis

To identify the coupling between hippocampal and LTL ripples, we tested whether the LTL ripple rates in the presence of hippocampal ripples were larger than in the absence of hippocampal ripples<sup>43,44</sup>. The hippocampus channels were paired with all LTL channels in each participant. For each hippocampal-LTL channel pair, we computed the hippocampal ripple peak-locked LTL ripple rate in a ([-0.5 s, 0.5 s]) time window. Additionally, non-ripple surrogates were derived for each channel pair, and the surrogate-locked LTL ripple rates were computed in time windows of the same length. Specifically, for all the *n* hippocampal ripples, we randomly selected *n* time points in the hippocampal channel with no ripple occurring 0.5 s before and after. Then, the LTL ripples were aligned to these non-ripple surrogates to obtain the surrogate-locked LTL ripple rates. This procedure was repeated 1000 times to generate a surrogate distribution, and empirical hippocampal ripple-locked LTL rates were z-scored relative to it, resulting in the normalized hippocampal-LTL coupled ripple indexes. The normalized hippocampal-LTL coupled ripple indexes were then averaged across all hippocampal-LTL channel pairs for each participant. Cluster-based permutation tests assessed whether normalized hippocampal-LTL coupling indexes exceeded zero within the  $\pm 0.5$  s window across participants. Significantly above-zero coupling index indicates hippocampal-LTL coupled ripples. This analysis was conducted across all task stages and within each of the task stages (i.e., encoding, maintenance, and retrieval).

### Multi-variate decoding of VSTM representations

To decode category-specific memory representations, we trained a linear support vector machine (SVM) to classify the four picture categories (animal, fruit, electrical device, furniture) from remembered and forgotten trials. The chance level for decoding was set at 25%. Inspired by prior studies showing that memory content is best captured by a broad range of spectral power<sup>78,79</sup>, we extracted broadband (2-180 Hz) spectral power from hippocampal and LTL channels. Time-frequency transformation was performed using complex Morlet wavelets (2-29 Hz in 1-Hz steps and 30-180 Hz in 5-Hz steps, 6 cycles), and all power spectral data were down-sampled to 100 Hz

after time-frequency transformation. Spectral power was z-scored for each frequency and channel across runs. To obtain time-resolved memory reactivation, decoding was performed in sliding time windows for both the training and test data, with a 400-ms window length and a 50-ms increment. To increase the signal-to-noise ratio, the spectral power was averaged across time points within each time window, resulting in frequency  $\times$  channel features as input to the SVM model. For each participant, normalized power from all hippocampus or LTL channels was used as input to the SVM. A leave-one-trial-out cross-validation was used to estimate decoding accuracy. SVMs were trained separately on each time window during encoding (yielding 60 decoders) and tested across all time windows of the task to assess temporal generalization. Decoding accuracy at each time point was statistically compared against the 25% chance level using the cluster-based permutation test.

### Coupled ripple-locked decoding accuracy

To assess whether memory reinstatement was linked to coupled ripples between the hippocampus and LTL, we computed decoding accuracy time-locked to coupled ripple events. First, coupled ripple events were identified separately for each hippocampal (HPC)-lateral temporal lobe (LTL) channel pair on individual trials. Coupled ripples were defined as temporally overlapping hippocampus and LTL ripples or those occurring within 50 ms of each other<sup>18</sup>. The peak time of each coupled event was set to the hippocampal ripple peak. The coupled ripple counts were then pooled across all trials and channel pairs within each participant, and subsequently averaged across participants. On average, each participant exhibited 439 (SD:125) coupled ripples in the VSTM task. When broken down by stage, each participant showed  $143 \pm 45$  coupled ripples during encoding,  $274 \pm 76$  during maintenance, and  $23 \pm 6$  during retrieval.

We then aligned trial-level decoding accuracy to these coupled ripple peaks, averaging values within a  $\pm 0.5$  s window to obtain the coupled-ripple-locked decoding accuracy. In addition to using the chance level (25%) as a baseline, we also generated decoding accuracy locked to non-coupled surrogate events as the alternative baseline. Specifically, for each of the coupled ripples, a corresponding time point without any coupled ripple activity within  $\pm 0.5$  s was randomly selected. This process was repeated 1000 times to produce a surrogate distribution. Empirical coupled ripple-locked decoding accuracy was z-scored relative to this distribution to obtain normalized decoding accuracy. Cluster-based permutation tests were used to assess whether normalized decoding accuracy exceeded zero.

As a control, we examined decoding accuracy locked to independent hippocampal or LTL ripples—i.e., ripples not overlapping or occurring within 50 ms of a ripple in the other region. Decoding accuracy for these independent ripples was z-scored relative to a non-ripple surrogate distribution, and the same statistical procedures were applied.

## Supplementary information

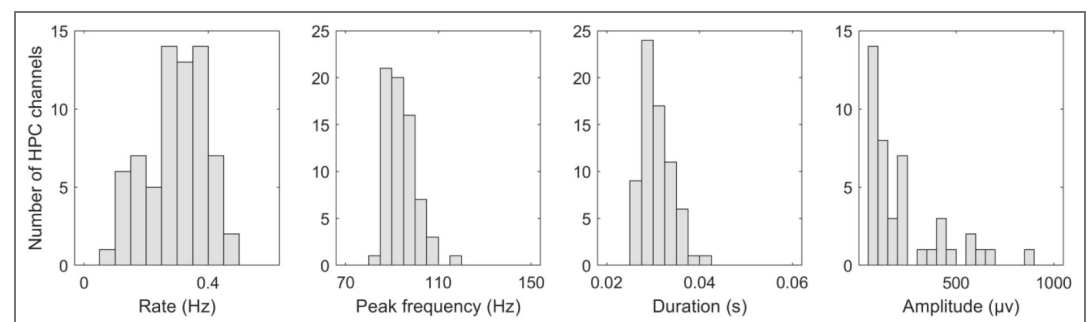


**Figure S1. Properties of ripples in HPC and LTL channels.** Distributions of ripple rate, peak frequency, duration, and amplitude across all HPC channels.

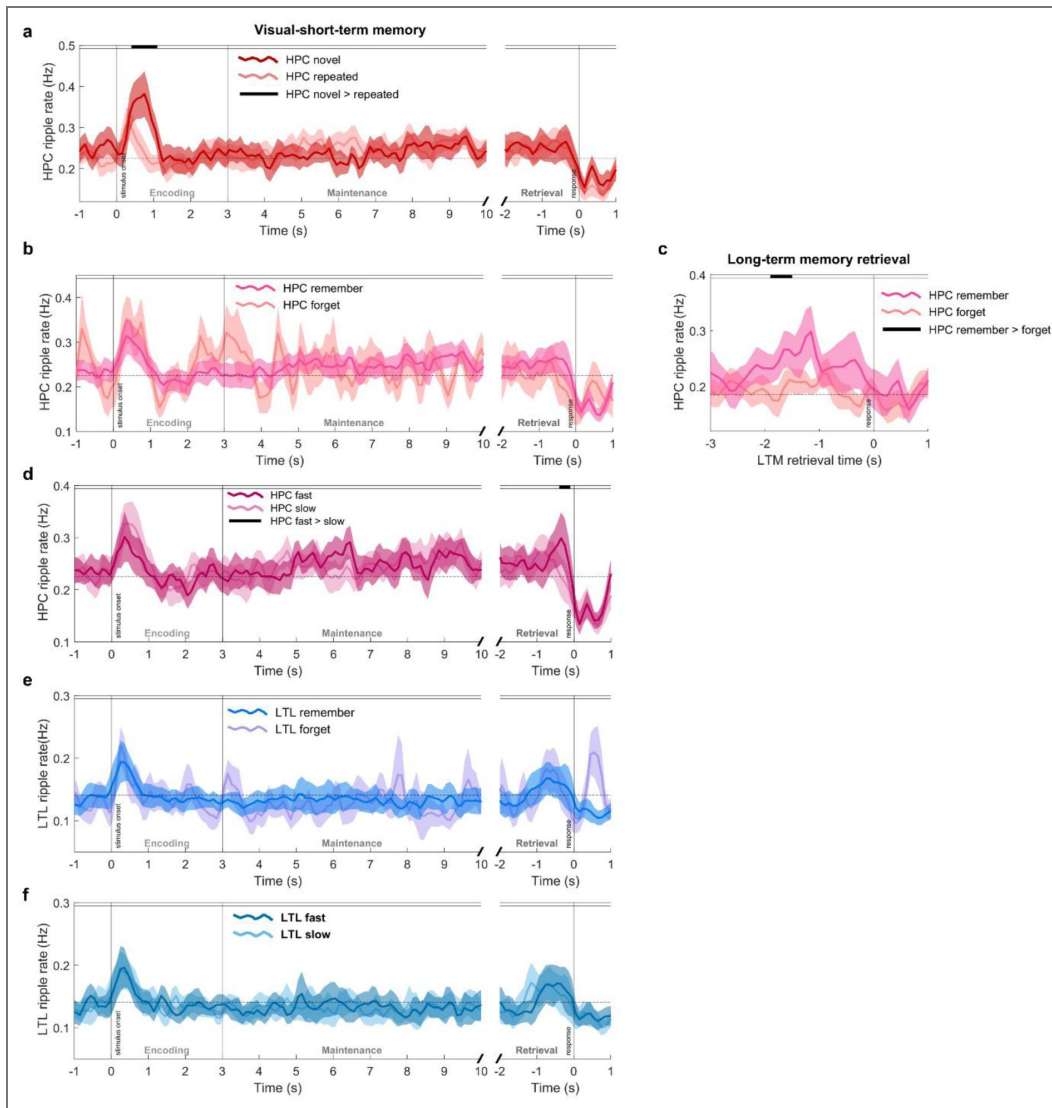


**Figure S2. Ripple rates in the hippocampus and lateral temporal lobe (LTL) during the visual short-term memory (VSTM) task and long-term memory (LTM) retrieval.**

(a) Time course of hippocampal ripple rates for novel (first presentation) and repeated (second and third presentations) trials. The black horizontal bar indicates a significant cluster (500–1100 ms post-stimulus) with higher ripple rates for novel versus repeated trials ( $p_{\text{cluster}} < 0.001$ ). (b) No significant differences were observed between hippocampal ripple rates for remembered and forgotten trials in any VSTM stage (all  $p_{\text{cluster}} > 0.466$ ). (c) Hippocampal ripple rates were significantly higher for LTM remembered than forgotten trials within a cluster (i.e., 1600–1900 ms before LTM retrieval responses) for remembered than forgotten trials ( $p_{\text{cluster}} = 0.047$ ). (d) Hippocampal ripple rates were significantly higher for fast compared with slow trials within a pre-response cluster (i.e., 150–450 ms before retrieval responses,  $p_{\text{cluster}} = 0.014$ ). (e) No significant differences were observed between LTL ripple rates of remembered versus forgotten trials in any VSTM stage (all  $p_{\text{cluster}} > 0.274$ ). (f) No significant differences were observed between hippocampal ripple rates for fast and slow remembered trials in any VSTM stage (all  $p_{\text{cluster}} > 0.237$ ). Shaded areas represent  $\pm$ SEM.

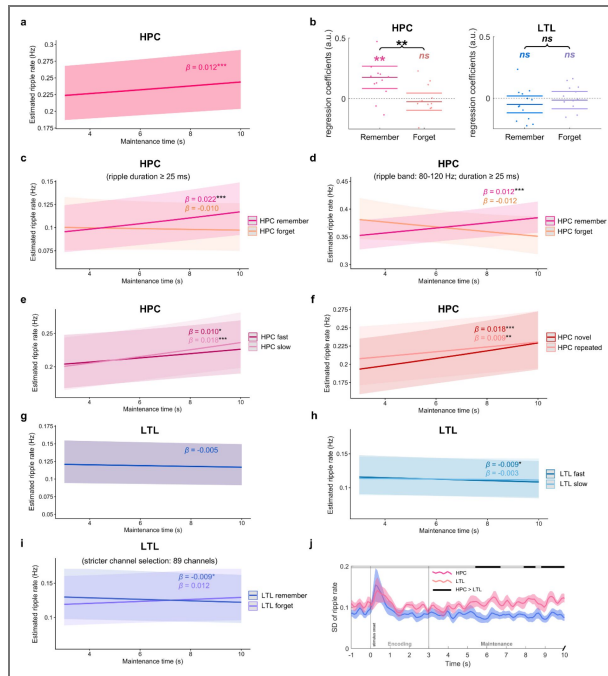


**Figure S3. Control analyses for the ripple ramping-up effects in the hippocampus (HPC) and lateral temporal lobe (LTL).**

(a) Significant ramping-up of hippocampal ripple rates during the maintenance period across all trials, channels, and participants ( $\beta = 0.012$ ,  $z = 4.678$ ,  $p < 0.001$ ). The y-axis shows model-estimated ripple rates. (b) Group-level analysis of the ripple ramping-up effects in the hippocampus and lateral temporal lobe (LTL). Left: for hippocampus, remembered trials showed significantly positive slopes ( $t(12) = 3.580$ ,  $p = 0.004$ ), whereas forgotten trials did not ( $t(12) = -0.669$ ,  $p = 0.516$ ). The slopes for remembered trials were significantly greater than those for forgotten trials ( $t(12) = 3.400$ ,  $p = 0.005$ ). Right: for the LTL, neither remembered trials ( $t(12) = -1.408$ ,  $p = 0.185$ ) nor forgotten trials ( $t(12) = -0.437$ ,  $p = 0.670$ ) of the visual short-term memory (VSTM) task showed significant slopes against zero. The slopes did not differ between VSTM remembered and forgotten trials ( $t(12) = -0.707$ ,  $p = 0.493$ ). (c) Control analyses by restricting hippocampal ripples (as detected in the main text) to those with a duration  $\geq 25$  ms, the results found a significant time  $\times$  VSTM accuracy interaction ( $\beta = 0.033$ ,  $z = 2.983$ ,  $p = 0.003$ ). Further analyses revealed a significant ramping-up of ripple rates over the maintenance period for remembered trials ( $\beta = 0.022$ ,  $z = 6.178$ ,  $p_{FDR} < 0.001$ ), but not for the forgotten items ( $\beta = -0.010$ ,  $z = -0.874$ ,  $p_{FDR} = 0.382$ ), consistent with Fig. 3a in the main text. (d) Control analyses for hippocampal ramping-up effect using an alternative frequency range (80-120 Hz) and detection criteria (duration  $\geq 25$  ms and peak amplitude  $> 3$  SD above baseline) following Vaz et al. (2019, *Science*). Our results found a significant time  $\times$  VSTM accuracy interaction was again observed ( $\beta = 0.024$ ,  $z = 3.281$ ,  $p = 0.001$ ). Further analyses revealed a significant ramping-up of ripple rates over the maintenance period for remembered trials ( $\beta = 0.012$ ,  $z = 4.998$ ,  $p_{FDR} < 0.001$ ), but not for the forgotten items ( $\beta = -0.012$ ,  $z = -1.648$ ,  $p_{FDR} = 0.099$ ), consistent with Fig. 3a in the main text. (e) Both fast and slow remembered trials showed significant hippocampal ramping-up effects (fast:  $\beta = 0.010$ ,  $z = 2.463$ ,  $p_{FDR} = 0.014$ ; slow:  $\beta = 0.018$ ,  $z = 4.625$ ,  $p_{FDR} < 0.001$ ), with no significant time  $\times$  retrieval speed interaction ( $\beta = 0.009$ ,  $z = 1.570$ ,  $p = 0.117$ ). The y-axis shows model-estimated ripple rates. (f) Both novel and repeated trials showed significant hippocampal ramping-up effects (novel:  $\beta = 0.018$ ,  $z = 4.00$ ,  $p_{FDR} < 0.001$ ; repeated:  $\beta = 0.009$ ,  $z = 2.973$ ,  $p_{FDR} = 0.003$ ), with no significant time  $\times$  novelty (novel vs. repeated) interaction effect ( $\beta = -0.009$ ,  $z = -1.716$ ,  $p = 0.086$ ). (g) Across all trials, channels, and participants, a linear mixed-effects model revealed a non-significant trend of decreasing LTL ripple rates during the maintenance period ( $\beta = -0.005$ ,  $z = -1.772$ ,  $p = 0.076$ ). The y-axis shows model-estimated ripple rates. (h) LTL ripple rates decreased significantly for the fast trials, with a similar but non-significant trend for the slow trials (fast:  $\beta = -0.009$ ,  $z = -2.245$ ,  $p_{FDR} = 0.049$ ; slow:  $\beta = -0.003$ ,  $z = -0.721$ ,  $p_{FDR} = 0.471$ ) and no significant time  $\times$  retrieval speed interaction ( $\beta = 0.006$ ,  $z = 1.087$ ,  $p = 0.277$ ). The y-axis shows model-estimated ripple rates. (i) Control analyses when restricting analyses to LTL bipolar channel pairs with at least one contact located within LTL gray matter or within 2 mm of gray matter ( $n = 89$  channels). The results revealed a significant time  $\times$  VSTM accuracy interaction was observed ( $\beta = -0.020$ ,  $z = -2.025$ ,  $p = 0.043$ ). Further analyses showed that this interaction was driven by a significant decrease in ripple rates for remembered items ( $\beta = -0.009$ ,  $z = -2.641$ ,  $p_{FDR} = 0.017$ ), whereas no significant effect was observed for forgotten trials ( $\beta = 0.012$ ,  $z = 1.134$ ,  $p_{FDR} = 0.257$ ). (j) The standard deviation of hippocampal ripple rates was significantly greater than that of LTL channels during the maintenance and pre-retrieval response periods across participants (all  $p_{s_{cluster}} < 0.032$ ), suggesting a greater heterogenous for hippocampal channels than LTL channels. Significant clusters are indicated by horizontal black bars. \*:  $p$  ( $p_{FDR}$ )  $< 0.05$ , \*\*:  $p$  ( $p_{FDR}$ )  $< 0.01$ , \*\*\*:  $p$  ( $p_{FDR}$ )  $< 0.001$ .

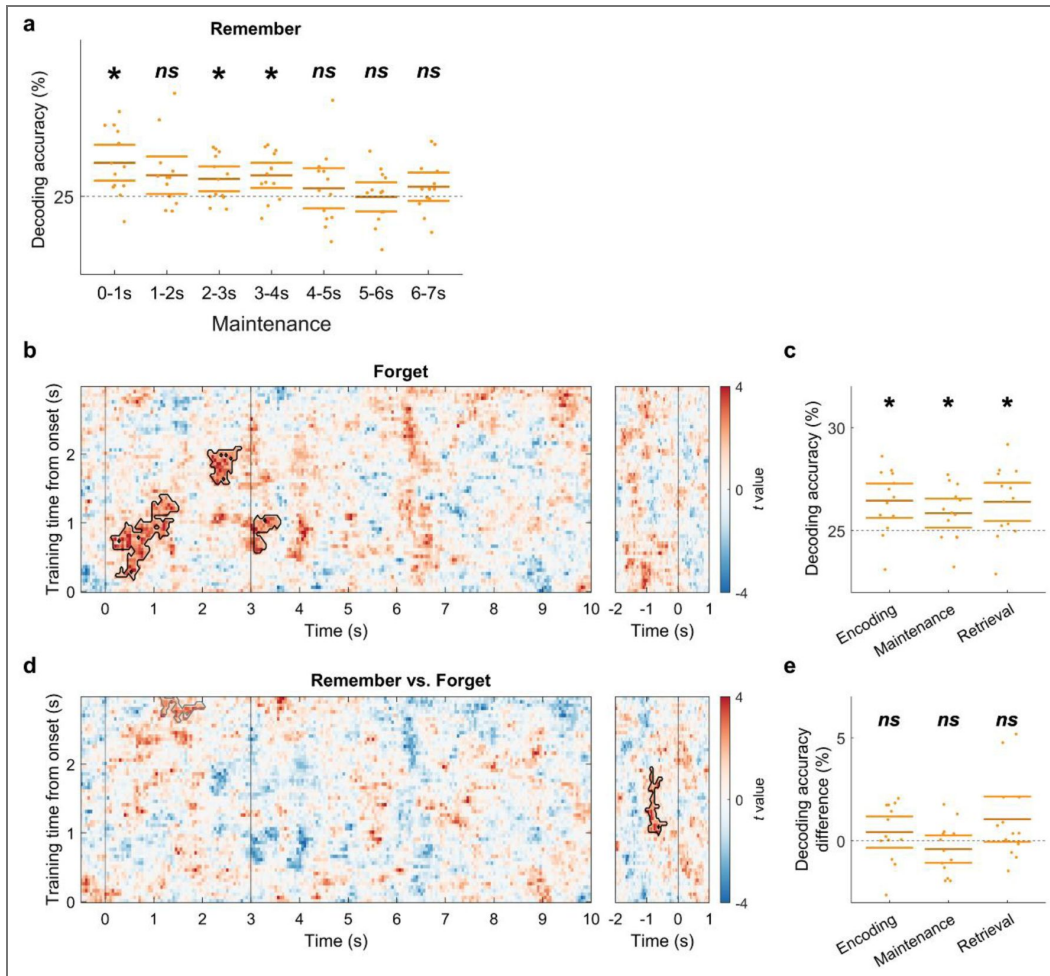


**Figure S4. Control analyses for decoding accuracy in the lateral temporal lobe (LTL) for remembered and forgotten trials.**

(a) Decoding accuracy was computed separately for each 1-s time bin of the maintenance period for remembered trials, with significant above chance (i.e., 25%) for the first, third, and fourth time bins ( $p_{\text{FDR}} < 0.042$ ). (b) Decoding accuracy of forgotten trials compared to chance level (25%) across the task (left: encoding and maintenance. Clusters showing significantly above-chance decoding accuracy are circled by black lines (all  $p_{\text{cluster}} < 0.028$ ). (c) Mean decoding accuracy across all time windows within each stage (encoding, maintenance, retrieval) was significantly above chance across participants (all  $p_{\text{FDR}} < 0.037$ ). (d) Decoding accuracy for VSTM remembered trials was significantly higher than for forgotten trials during retrieval in the cluster circled by black lines ( $p_{\text{cluster}} = 0.012$ ), with a similar trend but non-significant cluster during encoding ( $p_{\text{cluster}} = 0.064$ , circled by grey lines). (e) Mean decoding accuracy across all time windows within each stage did not differ significantly between VSTM remembered and forgotten trials (all  $p_{\text{FDR}} > 0.258$ ). \*:  $p_{\text{FDR}} < 0.05$ , ns: not significant.

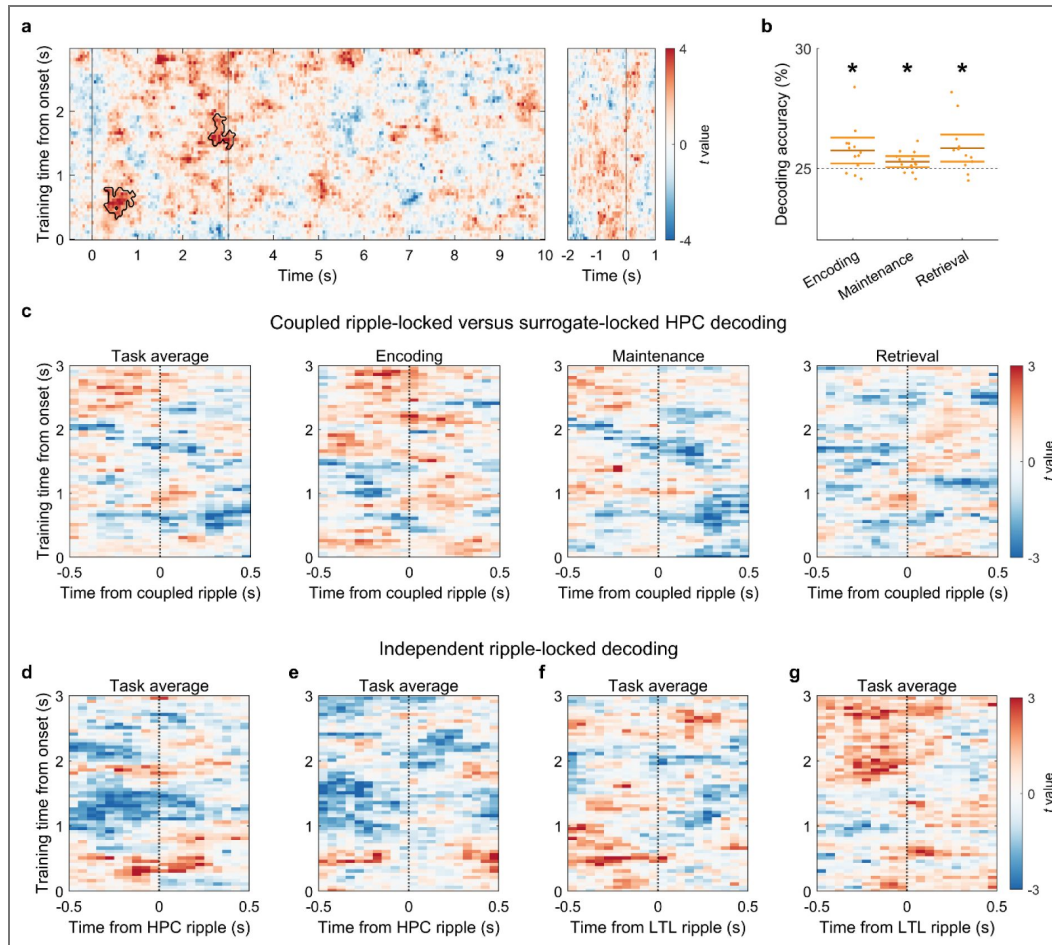


**Figure S5. Control analyses for coupled ripple-locked hippocampal memory reactivation or independent ripple-locked memory reactivation**

(a) HPC decoding accuracy compared to chance level (25%). Clusters indicate time windows with significantly above-chance decoding ( $p_{S_{cluster}} < 0.031$ ) and are circled by blacklines. (b) Averaged HPC decoding accuracies across all train-test time windows within individual task stages were all significantly above chance ( $p_{FDR} < 0.038$ ). (c) No significant clusters were found for HPC decoding accuracy locked to hippocampal-LTL coupled ripples across all task stages or within any task stage (all  $p_{S_{cluster}} > 0.470$ ). (d-e) Neither hippocampal (a) nor LTL (b) decoding accuracy was significantly locked to independent hippocampal ripples (all  $p_{S_{cluster}} > 0.222$ ). (f-g) Neither hippocampal (c) nor LTL (d) decoding accuracy was significantly locked to independent LTL ripples (all  $p_{S_{cluster}} > 0.203$ ). \*:  $p_{FDR} < 0.05$ .

**Figure S6. Control analyses for ruling out long-term memory (LTM) confounds in hippocampal ramping-up effects, coupled ripples, and ripple-locked memory reactivation.**

(a) Hippocampal ripples showed significant ramping-up effects for both subsequently LTM-remembered ( $\beta = 0.017$ ,  $z = 4.141$ ,  $p_{FDR} < 0.001$ ) and LTM-forgotten ( $\beta = 0.011$ ,  $z = 2.987$ ,  $p_{FDR} = 0.003$ ) trials, with no significant time  $\times$  LTM accuracy interaction ( $\beta = 0.003$ ,  $z = 0.439$ ,  $p = 0.661$ ). (b) Hippocampal-LTL coupled ripple rates did not differ between subsequently LTM remembered and forgotten trials ( $p_{s_{cluster}} > 0.626$ ). (c) Coupled ripple-locked memory reactivation also showed no significant difference between subsequently LTM remembered and forgotten trials (all  $p_{s_{cluster}} > 0.135$ ). \*\*:  $p_{FDR} < 0.01$ , \*\*\*:  $p_{FDR} < 0.001$ .

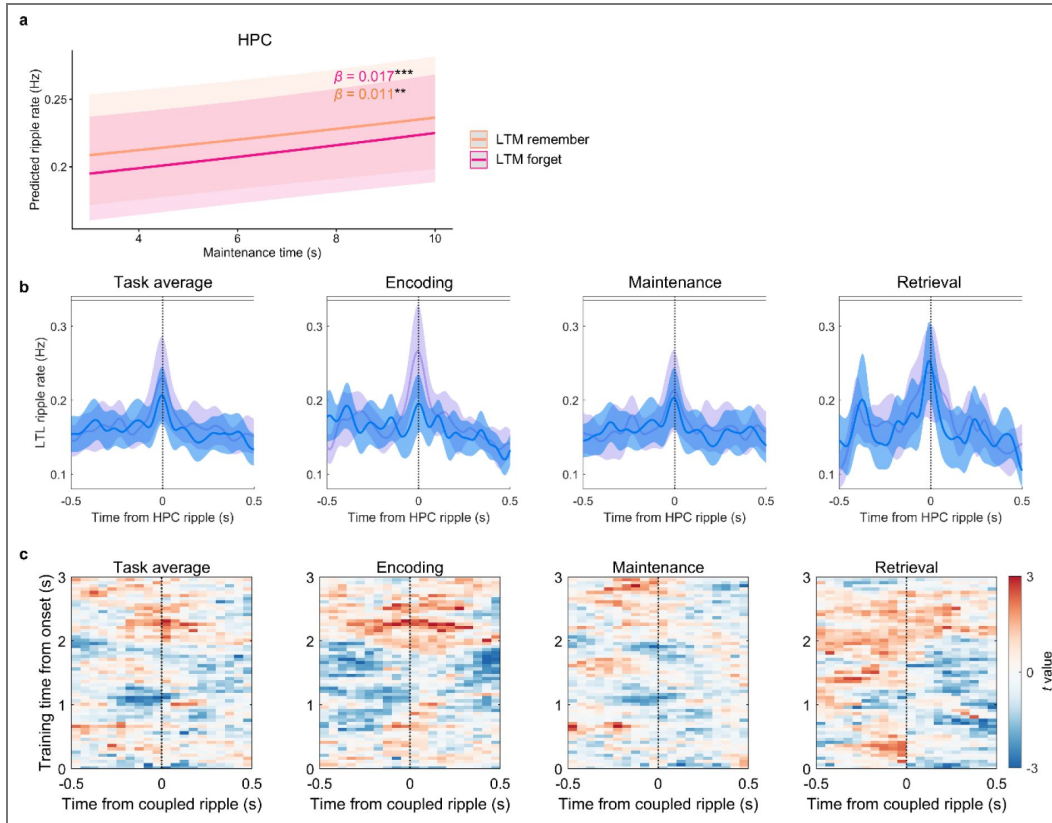


**Table S1. Participant-level summary of hippocampal channel counts and ramping-up coefficients ( $\beta$ ) for remembered and forgotten trials.**

Participant ID	Number of hippocampal channels	$\beta$ (remembered trials)	$\beta$ (forgotten trials)
1	2	-0.134	0.005
2	4	0.129	-0.047
3	2	0.179	-0.017
4	1	0.152	-0.041
5	2	0.471	0.147
6	2	0.209	0.115
7	8	0.503	-0.257
8	6	0.201	0.228
9	7	0.185	-0.041
10	4	0.262	-0.080
11	18	0.122	-0.075
12	1	-0.061	-0.240
13	12	0.060	-0.023

## Data availability

All preprocessed data are available on the Open Science Framework: <https://osf.io/gwe62/>. All custom MATLAB code necessary to reproduce the main conclusions of this study are available on the Open Science Framework: <https://osf.io/gwe62/2>. Any additional information required to reanalyze the data reported in this paper is available from the lead contact upon request.

## Acknowledgements

We thank the patients who volunteered to participate in the experiments and the support from our collaborators from Beijing Xuanwu Hospital, who provided the patient resources. This work was supported by the STI 2030-Major Projects (2021ZD0200401, 2021ZD0200409), the Fundamental Research Funds for the Central Universities (226-2024-00118), National Natural Science Foundation of China (32100851), and Guangdong Basic and Applied Basic Research Foundation (No. 2024A1515012667 and No. 2023A1515110311). This work was also supported by the grant from the Research Center for Brain Cognition and Human Development, Guangdong, China (No. 2024B0303390003).

## Additional information

### Author contributions

J.L. and G.X. conceived the original experiment. J.L., X.H., C.Y., N.A., S.Z., and Y.C. performed the analysis. J.L., X.H., and Y.C. wrote the initial manuscript. J.L., X.H., C.Y., N.A., G.X., S.Z., and Y.C. revised the manuscript.

### Funding

Funder	Grant reference number	Author
STI 2020-Major Projects	2021ZD0200401	Ying Cai
STI 2020-Major Projects	2021ZD0200409	Ying Cai
The Fundamental Research Funds for the Central Universities	226-2024-00118	Ying Cai
MOST   National Natural Science Foundation of China (NSFC)	32100851	Ying Cai
Guangdong Basic and Applied Basic Research Foundation	2024A1515012667	Jing Liu
Guangdong Basic and Applied Basic Research Foundation	2023A1515110311	Jing Liu
The Research Center for Brain Cognition and Human Development	2024B0303390003	Jing Liu

### Author ORCID iDs

Jing Liu:  <https://orcid.org/0000-0002-9167-6190>

Gui Xue:  <https://orcid.org/0000-0001-7891-8151>

Ying Cai:  <https://orcid.org/0000-0001-5125-2556>

## References

1. Scoville W.B., Milner B (1957) Loss Of Recent Memory After Bilateral Hippocampal Lesions. *J. Neurol. Neurosurg. Psychiatry* **20**:11-21 <https://doi.org/10.1136/jnnp.20.1.11> | PubMed

2. **Vargha-Khadem F.**, Gadian D.G., Watkins K.E., Connelly A., Van Paesschen W., Mishkin M. (1997) Differential Effects of Early Hippocampal Pathology on Episodic and Semantic Memory. *Science* **277**:376-380 <https://doi.org/10.1126/science.277.5324.376> | PubMed
3. **Squire L.R.**, Zola-Morgan S (1991) The Medial Temporal Lobe Memory System. *Science* **253**:1380-1386 <https://doi.org/10.1126/science.1896849> | PubMed
4. **Borders A.A.**, Ranganath C., Yonelinas A.P (2022) The hippocampus supports high-precision binding in visual working memory. *Hippocampus* **32**:217-230 <https://doi.org/10.1002/hipo.23401> | PubMed
5. **Li J.**, Cao D., Li W., Sarnthein J., Jiang T (2024) Re-evaluating human MTL in working memory: insights from intracranial recordings. *Trends Cogn. Sci* **28**:1132-1144 <https://doi.org/10.1016/j.tics.2024.07.008> | PubMed
6. **Ranganath C.**, D'Esposito M (2001) Medial Temporal Lobe Activity Associated with Active Maintenance of Novel Information. *Neuron* **31**:865-873 [https://doi.org/10.1016/s0896-6273\(01\)00411-1](https://doi.org/10.1016/s0896-6273(01)00411-1) | PubMed
7. **von Allmen D.Y.**, Wurmitzer K., Martin E., Klaver P. (2013) Neural activity in the hippocampus predicts individual visual short-term memory capacity. *Hippocampus* **23**:606-615 <https://doi.org/10.1002/hipo.22121> | PubMed
8. **Koen J.D.**, Borders A.A., Petzold M.T., Yonelinas A.P (2017) Visual short-term memory for high resolution associations is impaired in patients with medial temporal lobe damage. *Hippocampus* **27**:184-193 <https://doi.org/10.1002/hipo.22682> | PubMed
9. **Yonelinas A.P** (2013) The hippocampus supports high-resolution binding in the service of perception, working memory and long-term memory. *Behav. Brain Res* **254**:34-44 <https://doi.org/10.1016/j.bbr.2013.05.030> | PubMed
10. **Kamiński J.**, Sullivan S., Chung J.M., Ross I.B., Mamelak A.N., Rutishauser U (2017) Persistently active neurons in human medial frontal and medial temporal lobe support working memory. *Nat. Neurosci* **20**:590-601 <https://doi.org/10.1038/nn.4509> | PubMed
11. **Kornblith S.**, Quiroga R.Q., Koch C., Fried I., Mormann F (2017) Persistent Single-Neuron Activity during Working Memory in the Human Medial Temporal Lobe. *Curr. Biol* **27**:1026-1032 <https://doi.org/10.1016/j.cub.2017.02.013> | PubMed
12. **Xie W.**, Capiello M., Yassa M.A., Ester E., Zaghoul K.A., Zhang W (2023) The entorhinal-DG/CA3 pathway in the medial temporal lobe retains visual working memory of a simple surface feature. *eLife* **12**:e83365 <https://doi.org/10.7554/eLife.83365> | PubMed
13. **Buzsáki G** (2015) Hippocampal sharp wave-ripple: A cognitive biomarker for episodic memory and planning. *Hippocampus* **25**:1073-1188 <https://doi.org/10.1002/hipo.22488> | PubMed
14. **Eschenko O.**, Ramadan W., Mölle M., Born J., Sara S.J (2008) Sustained increase in hippocampal sharp-wave ripple activity during slow-wave sleep after learning. *Learn. Mem* **15**:222-228 <https://doi.org/10.1101/lm.726008> | PubMed
15. **Kunz L.**, Staresina B.P., Reinacher P.C., Brandt A., Guth T.A., Schulze-Bonhage A., Jacobs J (2024) Ripple-locked coactivity of stimulus-specific neurons and human associative memory. *Nat. Neurosci* **27**:587-599 <https://doi.org/10.1038/s41593-023-01550-x> | PubMed
16. **Norman Y.**, Yeagle E.M., Khuvis S., Harel M., Mehta A.D., Malach R (2019) Hippocampal sharp-wave ripples linked to visual episodic recollection in humans. *Science* **365**:eaax1030 <https://doi.org/10.1126/science.aax1030> | PubMed
17. **Sakon J.J.**, Kahana M.J (2022) Hippocampal ripples signal contextually mediated episodic recall. *Proc. Natl. Acad. Sci* **119**:e2201657119 <https://doi.org/10.1073/pnas.2201657119> | PubMed
18. **Vaz A.P.**, Inati S.K., Brunel N., Zaghoul K.A (2019) Coupled ripple oscillations between the medial temporal lobe and neocortex retrieve human memory. *Science* **363**:975-978 <https://doi.org/10.1126/science.aau8956> | PubMed

19. Zhang H., Skelin I., Ma S., Paff M., Mnatsakanyan L., Yassa M.A., Knight R.T., Lin J.J. (2024) Awake ripples enhance emotional memory encoding in the human brain. *Nat. Commun* **15**:215 <https://doi.org/10.1038/s41467-023-44295-8> | PubMed
20. Jadhav S.P., Kemere C., German P.W., Frank L.M. (2012) Awake Hippocampal Sharp-Wave Ripples Support Spatial Memory. *Science* <https://doi.org/10.1126/science.1217230> | PubMed
21. Zhang Y., Cao L., Varga V., Jing M., Karadas M., Li Y., Buzsáki G. (2021) Cholinergic suppression of hippocampal sharp-wave ripples impairs working memory. *Proc. Natl. Acad. Sci* **118**:e2016432118 <https://doi.org/10.1073/pnas.2016432118> | PubMed
22. Curtis C.E., D'Esposito M. (2003) Persistent activity in the prefrontal cortex during working memory. *Trends Cogn. Sci* **7**:415-423 [https://doi.org/10.1016/s1364-6613\(03\)00197-9](https://doi.org/10.1016/s1364-6613(03)00197-9) | PubMed
23. Fuster J.M., Alexander G.E. (1971) Neuron activity related to short-term memory. *Science* **173**:652-654 <https://doi.org/10.1126/science.173.3997.652> | PubMed
24. Harrison S.A., Tong F. (2009) Decoding reveals the contents of visual working memory in early visual areas. *Nature* **458**:632-635 <https://doi.org/10.1038/nature07832> | PubMed
25. Riggall A.C., Postle B.R. (2012) The Relationship between Working Memory Storage and Elevated Activity as Measured with Functional Magnetic Resonance Imaging. *J. Neurosci* **32**:12990-12998 <https://doi.org/10.1523/jneurosci.1892-12.2012> | PubMed
26. Axmacher N., Mormann F., Fernández G., Cohen M.X., Elger C.E., Fell J. (2007) Sustained neural activity patterns during working memory in the human medial temporal lobe. *J. Neurosci. Off. J. Soc. Neurosci* **27**:7807-7816 <https://doi.org/10.1523/jneurosci.0962-07.2007> | PubMed
27. Fiebig F., Lansner A. (2017) A Spiking Working Memory Model Based on Hebbian Short-Term Potentiation. *J. Neurosci. Off. J. Soc. Neurosci* **37**:83-96 <https://doi.org/10.1523/jneurosci.1989-16.2016> | PubMed
28. Miller E.K., Lundqvist M., Bastos A.M. (2018) Working Memory 2.0. *Neuron* **100**:463-475 <https://doi.org/10.1016/j.neuron.2018.09.023> | PubMed
29. Mongillo G., Barak O., Tsodyks M. (2008) Synaptic theory of working memory. *Science* **319**:1543-1546 <https://doi.org/10.1126/science.1150769> | PubMed
30. Stokes M.G. (2015) 'Activity-silent' working memory in prefrontal cortex: a dynamic coding framework. *Trends Cogn. Sci* **19**:394-405 <https://doi.org/10.1016/j.tics.2015.05.004> | PubMed
31. Lundqvist M., Herman P., Warden M.R., Brincat S.L., Miller E.K. (2018) Gamma and beta bursts during working memory readout suggest roles in its volitional control. *Nat. Commun* **9**:394 <https://doi.org/10.1038/s41467-017-02791-8> | PubMed
32. Spaak E., Watanabe K., Funahashi S., Stokes M.G. (2017) Stable and Dynamic Coding for Working Memory in Primate Prefrontal Cortex. *J. Neurosci. Off. J. Soc. Neurosci* **37**:6503-6516 <https://doi.org/10.1523/jneurosci.3364-16.2017> | PubMed
33. Axmacher N., Elger C.E., Fell J. (2008) Ripples in the medial temporal lobe are relevant for human memory consolidation. *Brain J. Neurol* **131**:1806-1817 <https://doi.org/10.1093/brain/awn103> | PubMed
34. O'Neill J., Pleydell-Bouverie B., Dupret D., Csicsvari J. (2010) Play it again: reactivation of waking experience and memory. *Trends Neurosci* **33**:220-229 <https://doi.org/10.1016/j.tins.2010.01.006> | PubMed
35. Rothschild G., Eban E., Frank L.M. (2017) A cortical-hippocampal-cortical loop of information processing during memory consolidation. *Nat. Neurosci* **20**:251-259 <https://doi.org/10.1038/nn.4457> | PubMed
36. Schreiner T., Griffiths B.J., Kutlu M., Vollmar C., Kaufmann E., Quach S., Remi J., Noachtar S., Staudigl T. (2024) Spindle-locked ripples mediate memory reactivation during human NREM sleep. *Nat. Commun* **15**:5249 <https://doi.org/10.1038/s41467-024-49572-8> | PubMed

37. **Khodagholy D.**, Gelineas J.N., Buzsáki G (2017) Learning-enhanced coupling between ripple oscillations in association cortices and hippocampus. *Science* **358**:369-372  
<https://doi.org/10.1126/science.aan6203> | PubMed
38. **Seger S.**, Ergit E., Arya S., Lega B (2025) Precise temporal dynamics of ripple events support order memory in human hippocampal–cortical circuits. *Proc. Natl. Acad. Sci* **122**:e2422266122  
<https://doi.org/10.1073/pnas.2422266122> | PubMed
39. **Pacheco Estefan D.**, Sánchez-Fibla M., Duff A., Principe A., Rocamora R., Zhang H., Axmacher N., and Verschure P.F.M.J. (2019) Coordinated representational reinstatement in the human hippocampus and lateral temporal cortex during episodic memory retrieval. *Nat. Commun* **10**:2255  
<https://doi.org/10.1038/s41467-019-09569-0> | PubMed
40. **Norman Y.**, Raccach O., Liu S., Parvizi J., Malach R (2021) Hippocampal ripples and their coordinated dialogue with the default mode network during recent and remote recollection. *Neuron* **109**:2767-2780. <https://doi.org/10.1016/j.neuron.2021.06.020> | PubMed
41. **Maris E.**, Oostenveld R (2007) Nonparametric statistical testing of EEG- and MEG-data. *J. Neurosci. Methods* **164**:177-190 <https://doi.org/10.1016/j.jneumeth.2007.03.024> | PubMed
42. **Verzhbinsky I.A.**, Rubin D.B., Kajfez S., Bu Y., Kelemen J.N., Kapitonava A., Williams Z.M., Hochberg L.R., Cash S.S., Halgren E (2024) Co-occurring ripple oscillations facilitate neuronal interactions between cortical locations in humans. *Proc. Natl. Acad. Sci* **121**:e2312204121  
<https://doi.org/10.1073/pnas.2312204121> | PubMed
43. **Ngo H.-V.**, Fell J., Staresina B (2020) Sleep spindles mediate hippocampal-neocortical coupling during long-duration ripples. *eLife* **9**:e57011 <https://doi.org/10.7554/eLife.57011> | PubMed
44. **Staresina B.P.**, Niediek J., Borger V., Surges R., Mormann F (2023) How coupled slow oscillations, spindles and ripples coordinate neuronal processing and communication during human sleep. *Nat. Neurosci* **26**:1429-1437 <https://doi.org/10.1038/s41593-023-01381-w> | PubMed
45. **Joo H.R.**, Frank L.M (2018) The hippocampal sharp wave–ripple in memory retrieval for immediate use and consolidation. *Nat. Rev. Neurosci* **19**:744-757 <https://doi.org/10.1038/s41583-018-0077-1> | PubMed
46. **Kikumoto A.**, Mayr U., Badre D (2022) The role of conjunctive representations in prioritizing and selecting planned actions. *eLife* **11**:e80153 <https://doi.org/10.7554/eLife.80153> | PubMed
47. **van Ede F.**, Chekroud S.R., Stokes M.G., Nobre A.C. (2019) Concurrent visual and motor selection during visual working memory guided action. *Nat. Neurosci* **22**:477-483  
<https://doi.org/10.1038/s41593-018-0335-6> | PubMed
48. **Lundqvist M.**, Rose J., Herman P., Brincat S.L., Buschman T.J., Miller E.K (2016) Gamma and Beta Bursts Underlie Working Memory. *Neuron* **90**:152-164 <https://doi.org/10.1016/j.neuron.2016.02.028> | PubMed
49. **Murray J.D.**, Bernacchia A., Roy N.A., Constantinidis C., Romo R., Wang X.-J (2017) Stable population coding for working memory coexists with heterogeneous neural dynamics in prefrontal cortex. *Proc. Natl. Acad. Sci* **114**:394-399 <https://doi.org/10.1073/pnas.1619449114> | PubMed
50. **Lundqvist M.**, Herman P., Miller E.K (2018) Working Memory: Delay Activity, Yes! Persistent Activity?. *Maybe Not. J. Neurosci. Off. J. Soc. Neurosci* **38**:7013-7019 <https://doi.org/10.1523/jneurosci.2485-17.2018> | PubMed
51. **Cowan N** (2019) Short-term memory based on activated long-term memory: A review in response to Norris. *Psychol. Bull* **145**:822-847 <https://doi.org/10.1037/bul0000199> | PubMed
52. **Trübtschek D.**, Marti S., Ojeda A., King J.-R., Mi Y., Tsodyks M., Dehaene S (2017) A theory of working memory without consciousness or sustained activity. *eLife* **6**:e23871  
<https://doi.org/10.7554/eLife.23871> | PubMed
53. **Athanasiadis M.**, Masserini S., Yuan L., Fetterhoff D., Leutgeb J.K., Leutgeb S., Leibold C (2024) Low rate hippocampal delay period activity encodes behavioral experience. *Hippocampus* **34**:422-437  
<https://doi.org/10.1002/hipo.23619> | PubMed

54. **Widloski J., Foster D.J.** (2025) Replay without sharp wave ripples in a spatial memory task. *Nat. Commun* **16**:10287 <https://doi.org/10.1038/s41467-025-65181-5> | [PubMed](#)
55. **de Voogd L.D., Fernández G., Hermans E.J.** (2016) Awake reactivation of emotional memory traces through hippocampal-neocortical interactions. *NeuroImage* **134**:563-572 <https://doi.org/10.1016/j.neuroimage.2016.04.026> | [PubMed](#)
56. **Gattas S., Larson M.S., Mnatsakanyan L., Sen-Gupta I., Vadera S., Swindlehurst A.L., Rapp P.E., Lin J.J., Yassa M.A.** (2023) Theta mediated dynamics of human hippocampal-neocortical learning systems in memory formation and retrieval. *Nat. Commun* **14**:8505 <https://doi.org/10.1038/s41467-023-44011-6> | [PubMed](#)
57. **Liu J., Zhang H., Yu T., Ni D., Ren L., Yang Q., Lu B., Wang D., Heinen R., Axmacher N., et al.** (2020) Stable maintenance of multiple representational formats in human visual short-term memory. *Proc. Natl. Acad. Sci* **117**:32329-32339 <https://doi.org/10.1073/pnas.2006752117> | [PubMed](#)
58. **Ramirez-Villegas J.F., Besserve M., Murayama Y., Evrard H.C., Oeltermann A., Logothetis N.K.** (2021) Coupling of hippocampal theta and ripples with pontogeniculooccipital waves. *Nature* **589**:96-102 <https://doi.org/10.1038/s41586-020-2914-4> | [PubMed](#)
59. **Cowan N.** (2001) The magical number 4 in short-term memory: A reconsideration of mental storage capacity. *Behav. Brain Sci* **24**:87-114 <https://doi.org/10.1017/s0140525x01003922> | [PubMed](#)
60. **Jeneson A., Squire L.R.** (2012) Working memory, long-term memory, and medial temporal lobe function. *Learn. Mem* **19**:15-25 <https://doi.org/10.1101/lm.024018.111> | [PubMed](#)
61. **Chung Y.H., Brady T.F., Störmer V.S.** (2024) Meaningfulness and familiarity expand visual working memory capacity. *Curr. Dir. Psychol. Sci* **33**:275-282 <https://doi.org/10.1177/09637214241262334>
62. **Bays P.M., Schneegans S., Ma W.J., Brady T.F.** (2024) Representation and computation in visual working memory. *Nat. Hum. Behav* **8**:1016-1034 <https://doi.org/10.1038/s41562-024-01871-2> | [PubMed](#)
63. **Brady T.F., Störmer V.S., Alvarez G.A.** (2016) Working memory is not fixed-capacity: More active storage capacity for real-world objects than for simple stimuli. *Proc. Natl. Acad. Sci* **113**:7459-7464 <https://doi.org/10.1073/pnas.1520027113> | [PubMed](#)
64. **Brady T.F., Störmer V.S.** (2022) The role of meaning in visual working memory: Real-world objects, but not simple features, benefit from deeper processing. *J. Exp. Psychol. Learn. Mem. Cogn* **48**:942-958 <https://doi.org/10.1037/xlm0001014> | [PubMed](#)
65. **Thibeault A.M.L., Stojanoski B., Emrich S.M.** (2024) Investigating the effects of perceptual complexity versus conceptual meaning on the object benefit in visual working memory. *Cogn. Affect. Behav. Neurosci* **24**:453-468 <https://doi.org/10.3758/s13415-024-01158-z> | [PubMed](#)
66. **Yu X., Thakurdesai S.P., Xie W.** (2025) Associating everything with everything else, all at once: Semantic associations facilitate visual working memory formation for real-world objects. *J. Exp. Psychol. Hum. Percept. Perform* **51**:1361-1373 <https://doi.org/10.1037/xhp0001347> | [PubMed](#)
67. **Daume J., Kamiński J., Schjetnan A.G.P., Salimpour Y., Khan U., Kyzar M., Reed C.M., Anderson W.S., Valiante T.A., Mamelak A.N., et al.** (2024) Control of working memory by phase-amplitude coupling of human hippocampal neurons. *Nature* **629**:393-401 <https://doi.org/10.1038/s41586-024-07309-z> | [PubMed](#)
68. **Verzhbinsky I.A., Daume J., Rutishauser U., Halgren E.** (2025) Cross-region neuron co-firing mediated by ripple oscillations supports distributed working memory representations. *Preprint at bioRxiv* <https://doi.org/10.1101/2025.09.04.674061> | [PubMed](#)
69. **Choo Y., Thakurdesai S.P., Qadri A., Fruchet O.E., Jackson S.N., Chatterjee R., Inati S.K., Zaghloul K.A., Xie W.** (2025) Medial temporal lobe lesions reduce visual working memory precision. *Brain J. Neurol. awaf* **397** <https://doi.org/10.1093/brain/awaf397> | [PubMed](#)
70. **Hitch G.J., Allen R.J., Baddeley A.D.** (2025) The multicomponent model of working memory fifty years on. *Q. J. Exp. Psychol* **78**:222-239 <https://doi.org/10.1177/17470218241290909> | [PubMed](#)

71. Liu J., Zhang H., Yu T., Ren L., Ni D., Yang Q., Lu B., Zhang L., Axmacher N., Xue G (2021) Transformative neural representations support long-term episodic memory. *Sci. Adv* **7**:eabg9715 <https://doi.org/10.1126/sciadv.abg9715> | PubMed
72. Ranganath C (2006) Working memory for visual objects: complementary roles of inferior temporal, medial temporal, and prefrontal cortex. *Neuroscience* **139**:277-289 <https://doi.org/10.1016/j.neuroscience.2005.06.092> | PubMed
73. Wu Z., Buckley M.J (2022) Prefrontal and Medial Temporal Lobe Cortical Contributions to Visual Short-Term Memory. *J. Cogn. Neurosci* **35**:27-43 [https://doi.org/10.1162/jocn\\_a\\_01937](https://doi.org/10.1162/jocn_a_01937) | PubMed
74. Chen Y.Y., Aponik-Gremillion L., Bartoli E., Yoshor D., Sheth S.A., Foster B.L (2021) Stability of ripple events during task engagement in human hippocampus. *Cell Rep* **35**:109304 <https://doi.org/10.1016/j.celrep.2021.109304> | PubMed
75. Oostenveld R., Fries P., Maris E., Schoffelen J.-M (2011) FieldTrip: Open Source Software for Advanced Analysis of MEG, EEG, and Invasive Electrophysiological Data. *Comput. Intell. Neurosci* **2011**:1-9 <https://doi.org/10.1155/2011/156869> | PubMed
76. Brown V.A (2021) An Introduction to Linear Mixed-Effects Modeling in R. *Adv. Methods Pract. Psychol. Sci* **4**:2515245920960351 <https://doi.org/10.1177/2515245920960351>
77. Benjamini Y., Hochberg Y (1995) Controlling the False Discovery Rate: A Practical and Powerful Approach to Multiple Testing. *J. R. Stat. Soc. Ser. B Stat. Methodol* **57**:289-300 <https://doi.org/10.1111/j.2517-6161.1995.tb02031.x>
78. Staresina B.P., Michelmann S., Bonnefond M., Jensen O., Axmacher N., Fell J (2016) Hippocampal pattern completion is linked to gamma power increases and alpha power decreases during recollection. *eLife* **5**:e17397 <https://doi.org/10.7554/eLife.17397> | PubMed
79. Yaffe R.B., Kerr M.S.D., Damera S., Sarma S.V., Inati S.K., Zaghoul K.A (2014) Reinstatement of distributed cortical oscillations occurs with precise spatiotemporal dynamics during successful memory retrieval. *Proc. Natl. Acad. Sci. U. S. A* **111**:18727-18732 <https://doi.org/10.1073/pnas.1417017112> | PubMed
- Jing Liu, Hui Zhang, Tao Yu, Duanyu Ni, Liankun Ren, Qin hao Yang, Baoqing Lu, Di Wang, Rebekka Heinen, Nikolai Axmacher, et al. (2020) sEEG-Memory. *Gui Xue*. ID yqftv <https://osf.io/yqftv/>

## Peer reviews

### Reviewer #1 (Public review):

Summary:

Cai et al. investigated the role of ripples in the hippocampus and coupled between the hippocampus and the neocortex in visual short-term memory (VSTM) using a similar lures match-to-sample task. The main findings are that hippocampal, but not neocortical ripples, ramp up during the maintenance period, peaking shortly before the memory response is given. This ramping-up effect was stronger for correct compared to incorrect trials. Furthermore, the authors show that stimulus category could be better decoded during coupled hippocampo-neocortical ripples compared to uncoupled ripples. These results provide compelling novel evidence for a role of ripples in supporting human visual short-term memory.

Strengths:

(1) State-of-the-art intracranial EEG in 13 patients during a well-designed visual short-term memory task, with simultaneous hippocampal and neocortical recordings.

(2) Thorough analysis pipeline with validation to detect ripple events, and distinguish them from spurious ripple activity (i.e., as induced by IEDs).

(3) Use of multivariate classifiers to resolve the neural representation of the stimuli.

Weaknesses:

It is difficult to find clear weaknesses in this paper, as the analyses are thorough, the results are clear, and the writing is excellent. However, some more sanity checks on the validity of ripples could have been conducted (i.e., making sure that ripple events have multiple peaks in the unfiltered raw signal at the ripple frequency). Also, the time window for coupled ripples appears to be a bit long, which makes it questionable to what degree these ripples are coupled (i.e., the time window is ~5 times longer than the duration of a ripple event). Lastly, the ramping-up effect could have been more clearly depicted in the figures, but that's a fairly minor point.

<https://doi.org/10.7554/eLife.111304.1.sa2>

## Reviewer #2 (Public review):

Summary:

Liu et al. record intracranial EEG from the hippocampus and lateral temporal lobe in thirteen neurosurgical patients while they perform a delayed match-to-sample visual short-term memory task. The central question is whether hippocampal sharp-wave ripples (brief high-frequency oscillations well established in the long-term memory consolidation literature) also contribute to the active maintenance of visual representations over a short delay. The authors report three main findings: hippocampal ripple rates progressively ramp up across the 7-second maintenance period, hippocampal ripples temporally co-occur with ripples in the lateral temporal lobe, and these coupled events coincide with above-chance category-level decoding of the memorized stimulus in the lateral temporal lobe. The findings are interpreted within the dynamic coding framework of working memory, which predicts discrete reactivation bursts rather than sustained firing during maintenance. The question is timely, and the use of intracranial recordings affords a level of temporal and spatial resolution unavailable to non-invasive methods.

Strengths:

The study addresses a genuinely important and underexplored question: whether a neural mechanism best characterized in the context of offline memory consolidation is also engaged during active online maintenance. The use of intracranial recordings in humans is well suited to this question, providing the millisecond temporal resolution and regional specificity needed to detect transient high-frequency events. The dissociation from long-term memory, tested by splitting remembered trials according to whether the item was later recalled in a cued-recall test, directly addresses what would otherwise be a significant confound, and the finding that ripple dynamics during maintenance are unrelated to subsequent long-term memory performance adds specificity to the interpretation. The coupled ripple analysis is methodologically grounded, and the finding that coupled but not isolated ripples coincide with elevated memory decoding is mechanistically informative. The multivariate decoding approach applied to lateral temporal lobe spectral power provides a meaningful index of memory reactivation that goes beyond simple univariate rate measures. The control analysis and the alternative ripple detection method provide useful robustness checks. The public availability of preprocessed data and analysis code on OSF is commendable.

Weaknesses:

(1) Theoretical motivation for examining ripples in visual short-term memory.

A fundamental question that the paper does not adequately address is why hippocampal ripples, a mechanism strongly associated with offline memory consolidation during sleep,

where they coordinate the transfer of hippocampal representations to cortex through temporally compressed replay, should be recruited for the online maintenance of visual information over a seconds-long delay. The Introduction acknowledges this gap but does not close it. The dynamic coding framework is used to motivate the ramping-up prediction, but this framework is agnostic about the specific neural mechanism responsible for reactivation bursts. In particular, the literature cited by the authors predicts high-frequency population activity or gamma bursts, but not specifically hippocampal ripples. The reasoning that "ripples share key properties with postulated reactivation bursts" risks being circular: it amounts to saying that ripples could be the relevant mechanism because the relevant mechanism has properties that ripples also have. A stronger theoretical motivation would require either evidence that the replay or reactivation computations that ripples support during offline states are also engaged during active short-term maintenance, or a mechanistic account of how the circuit processes underlying ripple generation are recruited differently across these two contexts.

This concern is compounded by what the authors present as one of their main controls. The finding that ripple dynamics during maintenance are not associated with subsequent long-term memory performance is treated as a reassurance that the observed effects are specific to short-term memory. But if ripples are canonically a long-term memory consolidation mechanism, the observation that they are engaged by a short-term memory task while appearing disengaged from concurrent long-term memory encoding is itself a finding that demands explanation. Resolving this tension is important for the paper's contribution to be correctly interpreted by the field.

#### (2) Ripple detection and specificity.

Even granting that ripples could in principle contribute to short-term memory maintenance, the study does not establish that the detected events are physiological sharp-wave ripples rather than broadband high-frequency activity. The detection band (70-180 Hz) substantially overlaps with the high-gamma range, which is a well-established proxy for local neural population activity and coding, and is broader than the 80-120 Hz band used by several of the cited papers, including Vaz et al. (2019), Ngo et al. (2020), Chen et al. (2021), Staresina et al. (2023), and Kunz et al. (2024). Without demonstrating that detected events have the hallmark features of physiological sharp-wave ripples, a clear narrowband spectral peak, and characteristic waveform morphology, it is difficult to conclude that the observed effects reflect a ripple-specific mechanism rather than a more general high-frequency population activity phenomenon. The reported mean rate of 0.29 Hz is somewhat higher than rates reported in some recent work, such as Chen et al. (2021, ref 74) and Kunz et al. (2024, ref 15). It is worth noting that van Schalkwijk and Helfrich (2026, Nature Communications) demonstrated that a large proportion of awake ripple detections in the human medial temporal lobe reflect false positives arising from aperiodic  $1/f$  noise, with task-related modulations of this noise floor producing spurious detections. The authors present an 80-120 Hz control analysis as a robustness check, but this inverts the appropriate logic: if 80-120 Hz is the more validated band, as the cited literature suggests, it should serve as the primary analysis rather than a supplementary one.

#### (3) Internal inconsistency with the dynamic coding framework.

The authors invoke the dynamic coding framework, which predicts that reactivation bursts should ramp up toward the end of the retention interval in the region where memory representations are actively maintained. The hippocampal ramping-up result is presented as confirming this prediction. However, the lateral temporal lobe, the region where above-chance category decoding is found and memory reactivation is attributed, shows no corresponding ramp-up. The authors acknowledge this asymmetry but do not offer a mechanistically satisfying explanation, and the suggestion that the effect might exist in unsampled subregions cannot be evaluated with the current data. This leaves the

framework's core prediction unconfirmed in the region that is claimed to maintain the representations.

(4) Coupled ripples, directionality of hippocampal-lateral temporal coupling, and the ramping-up paradox.

The conclusion that coupled hippocampal-lateral temporal ripples coordinate memory reactivation creates a logical tension that the paper does not resolve. If hippocampal ripples drive lateral temporal reactivation only when co-occurring with lateral temporal ripples, and hippocampal ripples ramp up in a memory-predictive fashion, then the absence of lateral temporal ripple ramping up implies that the hippocampal ramp-up is not primarily expressed through the coupled ripple mechanism, undermining the coherence of the two main findings. The coupled ripple analysis further quantifies only temporal co-occurrence and provides no evidence about the direction of influence. Without demonstrating that hippocampal ripples systematically precede lateral temporal ripples (i.e., the expected signature of hippocampus-to-cortex information flow), the central claim that hippocampal ripples drive lateral temporal reactivation remains an interpretive assumption. Directly testing whether lateral temporal ripples specifically coupled to hippocampal ripples show a ramping temporal profile during maintenance (even if overall lateral temporal ripple rates do not) is necessary to establish whether the lateral temporal lobe engages in hippocampally-gated reactivation bursts in the manner the framework predicts. Additionally, reporting the distribution of peak lags between hippocampal and lateral temporal ripple peaks, and testing whether hippocampal ripples systematically precede lateral temporal ripples, is similarly necessary to support the directional interpretation.

(5) Trial-level analysis clarity.

The paper reports that ripples occurred in 54%, 79%, and 27% of trials during encoding, maintenance, and retrieval, respectively, but does not state whether subsequent analyses were conducted on trials thresholded by ripple occurrence. Given that occurrence rates vary substantially across stages and conditions, this inclusion criterion has implications for interpreting rate differences and should be stated explicitly.

(6) Statistical model specification.

The methods describe the ramping-up analysis using both a "logistic" link function and a "Poisson link function" in different places, with the dependent variable described inconsistently as ripple occurrence and ripple count. These are not equivalent, and the distinction matters for interpreting the reported coefficients. Additionally, the regional dissociation in Figure 3 appears to be assessed by fitting separate models to each region and comparing results informally. This does not constitute a direct test of whether slopes differ between regions and risks the well-known error of inferring a difference based on one p-value being significant while another is not. A direct region  $\times$  time interaction test would more cleanly support the claimed dissociation.

<https://doi.org/10.7554/eLife.111304.1.sa1>

### Reviewer #3 (Public review):

Summary:

Liu, He, et al. present results suggesting hippocampal ripples support short-term working memory. The basic finding that hippocampal ripples increase during a 7s working memory maintenance period is intriguing and previously not shown as far as I know, but a lack of control analyses within the task, across brain regions, or as compared to alternative oscillatory signals makes the overall evidence weak. The author needs to more thoroughly

evidence this signal via several analyses (suggested below) to strengthen their finding. The paper moves on to a hippocampal-cortical ripple coupling analysis that needs further methodological details and corrected statistics to make a meaningful contribution. As is, the ripple coupling results don't seem to necessarily relate to the hippocampal ripples found in the maintenance period, making the manuscript somewhat incoherent and of low impact in its current form.

Major issues:


(1) The framing sets up "visual short term memory" (VSTM) and "long term memory" (LTM) as two different things. A long line of research with humans possessing MTL/hippocampus damage shows the hippocampal memory system contributes to working memory only when the task is difficult enough to warrant its recruitment (see Hannula et al. 2006 *J. of Neuroscience*, Pertzov et al. 2013 *Brain*, or particularly Jeneson et al. 2012 *Learning & Memory* and *J. of Neuroscience*). This theory therefore, suggests that the hippocampus contributes to working memory via LTM mechanisms, as opposed to it possessing two different roles (VSTM and LTM). While the authors might disagree with this framing, at a minimum, they should describe this line of work. As is, it's difficult to know how their task fits into this literature since it's a cross between a pattern separation probe (identify repeats from lures), working memory (7 s delays), and subsequent cued associate recognition. Addressing why they used this combination of task features would help frame its place in the literature.

(2) The basic idea of looking for hippocampal ripples as a marker for working memory maintenance is new, with no prior literature (that I know of in rodents or in the handful of human intracranial ripple papers) to build on. That said, I suspect hippocampal ripples act as a proxy for hippocampal activation, providing a possible explanation for the hippocampal ripple increase shown during the Maintenance period. The effect they show is well supported by the mixed effects modeling (MEM), making it a potentially meaningful finding, but considering the novelty, it's rather important that control analyses rule out alternative possibilities. I suggest two important ones and a third related to the lack of parametric manipulations in the next paragraph. First, the authors frame the paper by suggesting hippocampal ripples share features with beta/gamma burst theories of working memory maintenance. In that case, the obvious question is why use a ripple detector instead of measuring gamma (or beta) activity as in this previous work? Some work has suggested hippocampal ripples act differently than high-frequency activity (see Sakon et al. 2024 *J. of Neuroscience*), so an analysis contrasting ripples and gamma seems rather important. Second, and relatedly, the authors only compare the hippocampus and lateral temporal cortex (LTC), likely because these tend to be sites with strong coverage in epilepsy cases. That's ok, but typically there is also reasonable coverage in other MTL areas like entorhinal cortex and amygdala, which would serve as important controls to show what they're measuring likely relates to sharp-wave ripples (a hippocampal phenomenon) and not something more generic like gamma or HFA (as shown in Sakon et al. 2024, Howard et al. 2003 *Cerebral Cortex*, Axmacher et al. 2007 reference 26, Meltzer et al. 2008 *Cerebral Cortex*, etc.).

(3) Related to the last point, since there are no parametric manipulations (e.g., different delay durations, different set sizes, varying lure difficulties) there's no way to assess increased hippocampal ripples with stronger loads, which would be important for determining the hippocampal dependence of their task in the first place. Do the authors have any justification for this task as an assessment of hippocampal working memory? I could imagine using a top vs. bottom tercile of lure discrimination difficulty (as assessed across all participants or control non-patients) to compare hippocampal activity. But only after the first trial, each pair is used since only then would the patient have awareness of the difficulty of the upcoming

comparison. Or maybe something could be done by comparing VSTM performance by splitting patients based on how they performed at the LTM test.

(4) Also related to the VSTM vs. LTM framing, the authors use an "LTM" cued category recognition task--presumably done at the end of the repeat/lure recognition task--as a way to argue that the hippocampal ripple effects they see relate to VSTM and not LTM. The LTM task is disappointingly underdescribed, where even in the methods (lines 588-592) I cannot figure out when this task was probed, how many trials were done in comparison to the VSTM task, etc. Considering they use the LTM task to support their VSTM interpretation, it's rather crucial to understand precisely what they did. As is, the comparison they do present relies on a statistical error, where they compare p-values (n.b.

<https://www.nature.com/articles/nn.2886> ) instead of performing a direct interaction test (lines 177-180). Specifically, if they want to say their signal relates more to VSTM subsequent memory rather than LTM subsequent memory, they need to run a model of the form:  $\text{ripple\_rates} \sim \text{remembered} + \text{test\_type} + \text{remembered} * \text{test\_type}$  (where test\_type is either their VSTM or LTM task).

(5) As noted, the increase in hippocampal ripples during maintenance seems substantial, and the MEM confirms a significant increase over time. That said, the presentation of the data is atypical, with an example raster from one channel followed by average time courses of ALL participants below it. Why not show full raster plots for all participants? Ripples are so sparse that all the data in the task can be visualized in a single raster easily. A swarm plot indicating inter-patient variability in the maintenance signal also seems crucial. As is, there is no way to assess how much of the signal depends on a small subset of channels or patients.

(6) To compare ripple rates across task phases, they average over the bounds of each phase (lines 657-660) and input these into their MEMs. This approach makes sense for quantifying what we see in the ripple plots (Figure 2), except for Encoding, where they average over the entire 3 s window, even though there is clear tuning only from ~0-1 s. Using the tuned region and not the entire window is standard and would be more appropriate for the comparisons to maintenance, retrieval, etc (e.g., line 147-148 doesn't check out when looking at the figure), otherwise you are averaging over a seeming ripple inhibition from 1-2 s. They perform a cluster-based permutation test as is, so that a window or something a bit wider would be appropriate.

(7) The authors pivot to a hippocampal-cortical ripple coupling analysis to build the argument that the hippocampal ripples shown in Figure 2 support memory maintenance in the cortex. They use a window of -500 to 500 ms from hippocampal ripples to assess coupling. This is quite wide, since it doesn't seem plausible that a cortical ripple 500 ms from a hippocampal ripple means they synchronize. They cite two papers to justify the analysis, both of which use {plus minus}500 ms windows, but for spindle-ripple coupling, not ripple-ripple, so are miscited. Later in the paper, they switch to {plus minus}50 ms for another coupling analysis, raising the question of why they used {plus minus}500 ms in the previous analysis to begin with. If they want to claim cortical ripples are tuned by hippocampal ripples all the way up to 500 ms away, they should show the rasters (as in Figure 4a) and timecourse ripple rates, but going beyond {plus minus}500 ms to show that ripples in the {plus minus}50-500 ms range are above, say 500-1000 ms to justify their window selection. I will point out that there IS previous work that used {plus minus}500 ms to measure cortical-cortical ripple coupling (Dickey et al 2022 PNAS, which should be cited regardless, as I believe the first hippocampal-cortical ripple paper showing memory effects), although the figures in that paper suggest anything beyond {plus minus}250 ms returns to baseline (see Figure 2A-B).

(8) Lines 239 to 243 comparing p-values instead of an interaction test.

(9) I don't understand what "Further analysis based on the identified cluster" means (line 271). I see in Figure 5c that their broadband classifier identified a window of optimal

decoding, but did they use only activity in this cluster to train the subsequent classifier (Figure 5d)? If so, this is not described in the methods. And if it is done that way, I don't think the logic makes sense. As mentioned in comment 6, the ripples during encoding tune to 0-1s after image presentation. So it doesn't make sense to use a 1.85-2.25 s window for ripple-locked decoding—they should just be using the 0-1 s window (or whatever their cluster-based permutation test shows in Figure 2b). Otherwise, it would appear they are studying two different phenomena.

(10) As is, the results in Figure 5d need to be redone. First, the results described on lines 271-275 once again suffer from comparing p-values. They need to run an interaction model if they want to claim Maintenance shows stronger ripple-locked decoding than Encoding (it almost certainly will not, since Encoding appears to show some evidence of decoding ( $p=0.118$ )). Second, even if they do change the framing to say Encoding and Maintenance show significant decoding, is it meaningful if Retrieval fails to? If you cannot decode the same information at the time of retrieval as is theoretically being held in working memory during the delay, the coupled ripple reactivation story wouldn't appear to make sense. They do show significant Retrieval decoding in Figure 5a-b, but since I don't really understand how they settled on the "identified cluster" in Figure 5c, I'm not sure what to make of the difference between these decoders.

(11) Finally, as mentioned in the summary, the analyses in Figures 2-3 seem disjointed from those in Figures 4-5. Part of this has to do with the switch to a broadband classifier, then a switch back to coupled ripples, and then, as I already mentioned, decoding results with time windows that don't align with the hippocampal ripple effects they showed earlier. Further, since the main point of Figures 2-3 is to establish a ramp in hippocampal ripples across maintenance, shouldn't they be trying to show how the decoding changes over the course of the Maintenance period? It would also help the interpretation of Figure 5 to see how the coupled ripples change over time in Figure 4 (as they showed them in Figure 2).

Minor issues:

(1) Instead of citing a software package like Emmeans, the statistical test being performed should be explained.

(2) Decoding % accuracy in the heatmaps in Figure 5 and supplementary would be more intuitive, particularly since Figure 5b uses accuracy anyway.

(3) Figure 2b is misleading with an unnecessary change in the y-axis for retrieval.

(4) In Figure 2d, a significant cluster is mentioned, but not drawn onto the figure as in Figure 2b.

<https://doi.org/10.7554/eLife.111304.1.sa0>